Fluorescence signals from the Mg^{2+}/Ca^{2+} indicator furaptra in frog skeletal muscle fibers

M. Konishi, N. Suda, and S. Kurihara
Department of Physiology, The Jikei University School of Medicine, Tokyo 105, Japan

ABSTRACT The fluorescent Mg^{2+}/Ca^{2+} indicator, furaptra, was injected into single frog skeletal muscle fibers, and the indicator's fluorescence signals were measured and analyzed with particular interest in the free Mg^{2+} concentration ($[Mg^{2+}]$) in resting muscle. Based on the fluorescence excitation spectrum of furaptra, the calibrated myoplasmic $[Mg^{2+}]$ level averaged 0.54 mM, if the value of dissociation constant (K_D) for Mg^{2+} obtained in vitro (5.5 mM) was used. However, if the indicator reacts with Mg^{2+} with a two-fold larger K_D in myoplasm, as previously suggested for the furaptra-Ca^{2+} reaction (M. Konishi, S. Hollingworth, A. B. Harkins, S. M. Baylor. 1991. *J. Gen. Physiol.* 97:271–301), the calculated $[Mg^{2+}]$ would average 1.1 mM. Thus, the value 1.1 mM probably represents the best estimate from furaptra of $[Mg^{2+}]$ in resting muscle fibers. Extracellular perfusion of muscle fibers with high Mg^{2+} concentration solution or low Na^+ concentration solution did not cause any detectable changes in the $[Mg^{2+}]$-related furaptra fluorescence within 4 min. The results suggest that the myoplasmic $[Mg^{2+}]$ is highly regulated near the resting level of 1 mM, and that changes only occur with a very slow time course.

INTRODUCTION

Intracellular free Mg^{2+} concentration plays an essential role in numerous cell processes of many cell types (for review, see Flatman, 1984). In skeletal muscle fibers, the free Mg^{2+} concentration ($[Mg^{2+}]$) in myoplasm probably influences muscle contraction via many different pathways: (*a*) Ca^{2+} release from the sarcoplasmic reticulum (SR) (for review, see Endo, 1977), (*b*) the Ca^{2+}-tension relation of the myofilaments (e.g., Donaldson and Kerrick, 1975), (*c*) the turn-over rate of the SR Ca^{2+} pump (for review, see Inesi, 1985), (*d*) Ca^{2+} binding to the Ca^{2+}-Mg^{2+} binding sites on parvalbumin (Gillis et al., 1982). It is, therefore, possible that the level of myoplasmic $[Mg^{2+}]$ plays a regulatory role in muscle function in various experimental conditions.

Due to the significance of Mg^{2+} in myoplasm, many attempts have been made to estimate the $[Mg^{2+}]$ level using various methods, such as intracellular optical indicators (arsenazo III, antipyrylazo III, arsenazo I, dichlorophosphonazo III) (Baylor et al., 1982; Baylor et al., 1986), Mg^{2+}-sensitive microelectrodes (Hess et al., 1982; Alvarez-Leefmans et al., 1986) and nuclear magnetic resonance (for review, Gupta and Gupta, 1984). However, the estimated $[Mg^{2+}]$ values vary between 0.2 and 6 mM.

Furaptra, a fluorescent Mg^{2+}/Ca^{2+} indicator (also called mag-fura-2), undergoes large fluorescence intensity changes upon binding to Mg^{2+} or Ca^{2+} probably with 1:1 stoichiometry (Raju et al., 1989). When furaptra is injected into myoplasm, its fluorescence signals can be detected for a relatively long period of time (Konishi et al., 1991). The main drawback of furaptra as a Mg^{2+} indicator is its sensitivity to Ca^{2+} (K_D of furaptra for Mg^{2+} and Ca^{2+} are 5.5 mM and 44 μM, respectively, at 16°C). Furaptra fluorescence signals were, therefore, thought to mostly reflect $[Mg^{2+}]$ in resting fibers, but actually they primarily reflect the change in free Ca^{2+} concentration ($\Delta[Ca^{2+}]$) during muscle activity (Konishi et al., 1991). The Ca^{2+}-related signal makes it very difficult to monitor $[Mg^{2+}]$ changes during muscle activity.

We have studied furaptra's fluorescence signals in frog skeletal muscle fibers to obtain a better estimate of $[Mg^{2+}]$ at rest. The optical apparatus previously used in this laboratory (Suda and Kurihara, 1991) was modified to measure the intrinsic absorbance of a muscle fiber (before the indicator injection) and the indicator's fluorescence intensity. The first part of this article describes the measurements of intrinsic absorbance in the near UV (340 to 400 nm). Since fiber diameters are typically large (100–200 μm), a nonnegligible fraction of the excitation light beam is absorbed by the muscle fiber, which in turn causes attenuation of the fluorescence intensity.

Secondly, the indicator's fluorescence excitation spectrum was measured in fibers at rest, and the analysis included a correction for the fiber's intrinsic absorbance obtained in the same portion of the muscle fiber. From the estimate of the Mg^{2+}-bound fraction of the indicator in the resting fibers, the $[Mg^{2+}]$ level was calibrated. Considering the possibility that furaptra reacts with Mg^{2+} with an altered K_D in myoplasm, the best estimate from furaptra of $[Mg^{2+}]$ in resting muscle fibers averaged 1.1 mM. This value is in the range of the recent values obtained by other methods (Gupta and Gupta, 1984; Blatter, 1990).

Finally, we studied the change in myoplasmic $[Mg^{2+}]$ by two experimental maneuvers, high extracellular Mg^{2+} concentration (20 mM) and low extracellular Na^+ concentration (2 mM). Recently, work with a Mg^{2+}-sensitive microelectrode (Blatter, 1990) has suggested that myoplasmic $[Mg^{2+}]$ can change rapidly and reversi-

Address correspondence to Dr. Masato Konishi, Department of Physiology, The Jikei University School of Medicine, 3-25-8 Nishi-shinbashi, Minato-ku, Tokyo 105, Japan

bly in high extracellular [Mg^{2+}] or low [Na^+]. In contrast to our expectation that furaptra's fluorescence signals would change in a rapid and reversible fashion to these maneuvers (Blatter, 1990), neither of these interventions produced a detectable change in [Mg^{2+}]-related furaptra fluorescence within 4 min. A few hours of exposure to high extracellular [Mg^{2+}] caused only a very slight change in the furaptra's fluorescence signals, which could be interpreted as an increase of myoplasmic [Mg^{2+}].

A part of the data has been published in abstract form (Konishi et al., 1992).

METHODS

Single twitch fibers were dissected from the tibialis anterior muscle (or occasionally the semitendinosus muscle) of frogs (*Rana temporaria*), mounted horizontally in the muscle chamber on the stage of an inverted microscope (see below), and slightly stretched to sarcomere length 2.8 μm by observation of laser diffraction lines. The temperature of the perfusing solution was maintained at 16–17°C. Furaptra was injected into myoplasm from a micropipette tip containing 10–20 mM indicator in a buffer solution (see below) by applying pressure (3–10 kg/cm^2) to the back of the pipette; the micropipette was then withdrawn and furaptra's fluorescence intensity in myoplasm was measured. When the fluorescence signals were measured during muscle activity, the muscle fiber was further stretched to a sarcomere length of 3.6–3.8 μm to reduce the movement artifact in the fluorescence signals. For electrical stimulation, brief (500 μs) supra-threshold pulses were applied through a pair of platinum-black electrodes placed parallel to the whole length of the muscle fiber, and developed tension was measured by a semiconductor transducer (Kulite, New Jersey) attached to one end of the muscle fiber. Fiber viability was occasionally checked during the experiments by applying 1 s 50 Hz stimuli. Only fibers that showed complete tetanic tension with a sustained plateau were included in the analysis.

Solutions and chemicals

The normal Ringer's solution contained (mM): 115 NaCl, 2.5 KCl, 1.8 $CaCl_2$, and 5 MOPS (3-[*N*-morpholino]propanesulfonic acid), pH 7.05 (titrated with 2.3 mM NaOH). The fiber dissection and the optical measurements were carried out in normal Ringer's solution, unless otherwise stated. For the experiments in which fibers were exposed to high extracellular Mg^{2+} and/or low Na^+ concentrations, the Ringer's solution was modified as indicated, while maintaining osmolality at 240 ± 5 mosm/kg H_2O (Osmotron-20 osmometer, Orion Research Inc., Massachusetts):

(*a*) *High Mg^{2+}-Ringer's solution.* 20 mM $MgCl_2$ was added, while NaCl concentration was reduced to 90 mM.

(*b*) *Low Na^+/Li^+-Ringer's solution.* 115 mM NaCl was replaced by 100 mM LiCl plus 10 mM $MgCl_2$.

(*c*) *Low Na^+/TMA^+-Ringer's solution.* 115 mM NaCl was replaced by 100 mM TMA-Cl (tetramethylammonium chloride) plus 10 mM $MgCl_2$.

For intracellular acidosis experiments, normal Ringer's solution, titrated (with NaOH) to pH 7.40 and bubbled vigorously with a mixture of 5% CO_2/95% room air, was used in replacement of a CO_2-free normal Ringer's solution titrated to pH 7.40. For these experiments the muscle fibers were equilibrated for at least 3 h in the CO_2-free Ringer's solution before imposition of the acid load.

For intracellular injection, furaptra (tetra-potassium salt), at a final concentration of 10–20 mM, was dissolved in a buffer solution containing 120 mM KCl and 10 mM PIPES (piperazine-*N,N'*-bis[2-ethanesulfonic acid], K salt) (pH 7.0); the buffer solution was passed through a chelex column to minimize contamination by Ca^{2+} and other metal ions. The $MgCl_2$ injection solution contained 50 mM $MgCl_2$ and 5 mM PIPES (K salt), with pH adjusted to 7.0. Ca^{2+} contamination in this solution was checked by atomic absorption spectrophotometry, and found to be less than 3 μM. For the injection of EDTA (ethylenediamine-*N,N'*-tetraacetic acid), 30 mM EDTA was dissolved in H_2O and titrated (with KOH) to pH 7.0.

Furaptra (tetra-potassium salt) was purchased from Molecular Probes Inc. (Eugene, OR) as mag-fura-2 (lot No. 9A). Furaptra of this particular lot did not seem to be entirely pure, as judged from the presence of a slight secondary spot on the thin layer chromatograph (on silica with butanol-acetic acid-water 4:1:1). For consistency, all in vitro and in vivo measurements were carried out with the same lot (9A) to minimize the potential influence of impurity. Fura-2 (penta-potassium salt) was also purchased from Molecular Probes Inc. For the titrations with Mg^{2+}, newly purchased crystals of $MgCl_2$:$6H_2O$ (Kanto Chemical Co., Tokyo) were used. For the Ca^{2+} titration, a certified 1 M $CaCl_2$ solution was used (BDH Chemicals Ltd., Poole, UK).

Optical set-up and data collection

As shown in Fig. 1, an inverted microscope (Diaphot TMD; Nikon, Tokyo) was equipped with epi-illumination optics and a dual wavelength fluorometer (CAM 230; JASCO, Tokyo), that could alternately switch two excitation wavelengths (switching frequency up to 1 KHz). Light emitted from a Xe arc lamp (150 W, not shown in Fig. 1) was fed in parallel into two independent monochrometers (not shown) to obtain quasi-monochromatic light beams (half width 5 or 10 nm) of two different incident wavelengths, λ_1 and λ_2 (variable in wavelength range 300–700 nm). Either λ_1 and λ_2 were switched at 100 Hz (dual-wavelength excitation), or else only λ_1 was used continuously (single-wavelength excitation). The pulse-controlled shutter (S1) was opened only when the optical measurements were made, in order to minimize the period of fiber illumination. The incident light (λ_1 or λ_2), passed through a fiber optic probe (OP), was reflected by a dichroic mirror (DM) and was focused on the muscle fiber (mf) on the microscope stage by a UV-transmissive, high NA objective (obj1), which also collected the emitted fluorescence from the muscle fiber. The fluorescence at 500 nm (±20 nm) was selected by an interference filter (F1) and detected by a photomultiplier tube (PMT). An additional detector unit was positioned above the muscle fiber in the path of the incident light beam. The light beam transmitted by the muscle fiber passed through a filter (F2) that blocked fluorescence (see next paragraph), and was focused by a quartz lens (obj2) onto a photodiode (PD). This apparatus was used for optical measurements of the following three types:

Absorbance mode (single-wavelength excitation). An aperture diaphragm (D2) was inserted into the back of the objective (obj1) to limit the NA of the incident light to 0.3–0.4 and a slit was inserted into position D1 to reduce the field of illumination to a rectangular window on the muscle fiber. At the position of the muscle fiber, the size of the window (length along fiber axis and width) was 650 μm and 30–50 μm, respectively. The window width was selected in proportion to the fiber diameter. The transmitted light was detected by a photo-diode detector set above the muscle fiber through a blocking filter (either a wide-band UV transmission filter or a 400 nm interference filter for the incident wavelength at 340–375 or 400 nm, respectively), and the voltage output of the photo-diode was displayed on a digital voltmeter. The bandwidth of the incident light beam was 10 nm.

Fluorescence mode 1. To measure fluorescence spectra, the optical configuration was very similar to that of absorbance mode, except that the square slit (D1) was removed (single-wavelength excitation, bandwidth of incident light 5 nm). Although the presence of the aperture diaphragm (D2) renders it clearly disadvantageous for fluorescence measurements (since fluorescence intensity was reduced by an order of magnitude), we limited the NA of the objective to the same value used for the measurements of the intrinsic absorbance, so that the excitation spectra could be corrected for the effects of fiber absorbance (see below).

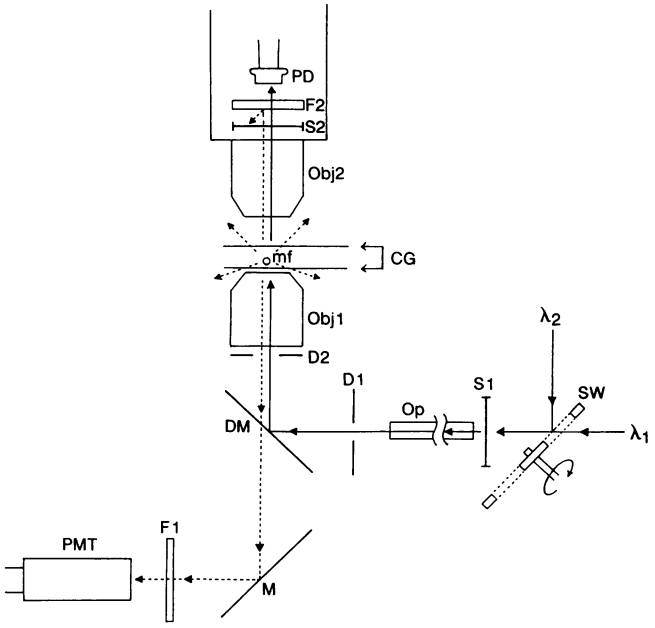

FIGURE 1 A schematic drawing of the experimental set-up for absorbance and fluorescence measurements using an inverted microscope. Solid arrows indicate the path of incident or transmitted light; dotted arrows indicate the path of fluorescence light. λ_1 and λ_2, light beams of two different wavelengths. S1, an electronic shutter for the incident light beam. Op, quartz optic fibers for light guide. D1, a slit for absorbance measurements. DM, a dichroic mirror which reflects light (wavelength $\leq$ 400 nm) towards D2, an aperture diaphragm which limits NA of the objective (obj1) to 0.3–0.4. Obj1, an objective (Fluor 20; magnification, 20×; NA, 0.75; Nikon, Tokyo, Japan). mf, a muscle fiber. CG, thin cover glasses (thickness 0.18 mm; Matsunami Glass Ind. Ltd., Tokyo, Japan). Obj2, an objective with a single quartz lens (magnification 4.6×, NA 0.37; Meiritsu Seiki, Tokyo, Japan). S2, an electronic shutter. F2, a blocking filter to eliminate fluorescent light (UV-360, half transmission 330–370 nm; Hoya Glass, Tokyo, Japan). PD, photodiode (S1226-8BQ; Hamamatsu Photonics, Hamamatsu, Japan). M, a mirror. F1, an emission filter (S40-500-F, peak transmission at 500 nm, halfwidth 40 nm, Corion Co., MA.) PMT, a photomultiplier tube (R268; Hamamatsu Photonics). For simplicity, only two of the objective lenses in the optical path are shown.

Fluorescence mode 2. For the measurements of the fluorescence intensity change (as opposed to the resting absolute intensity value) no correction was made for the intrinsic absorbance of the fiber. In this case, both the square slit (D1) and the aperture diaphragm (D2) were removed to maximize the S/N ratio. The bandwidth of the incident light was 5 nm. For the measurements of changes on a millisecond time scale (e.g., the Ca signal in Fig. 9), single-wavelength excitation was selected. In the other cases, the fluorescence intensities excited at λ_1 (350 nm) and λ_2 (380 nm) were alternately measured (dual-wavelength excitation) at a switching frequency of 100 Hz.

The output current of the photomultiplier tube was linearly converted to voltage, and the voltage signals when excited at λ_1 and at λ_2 were separated by a peak-hold circuit. (The peak-hold circuit was bypassed when single-wavelength excitation was selected.) The voltage outputs were amplified, low pass filtered (8 pole Bessel filter), and simultaneously sampled by a 12-bit analogue-to-digital converter with a sample-and-hold circuit. The cut-off frequency of the Bessel filter (f_c) and the sampling rate of analogue-to-digital conversion (f_s) were usually 10 Hz except for the $\Delta[Ca^{2+}]$ measurements, in which f_c and f_s were 1 KHz and 3 KHz, respectively. Signals from up to four channels were collected: fluorescence intensity excited at λ_1 and at λ_2, change in fiber tension and the electrical stimulus applied to the muscle fiber. The sampled data were stored and analyzed with a personal computer (PC-9801 RA21; NEC, Tokyo).

In vitro fluorescence measurements

In vitro fluorescence measurements were carried out on the inverted microscope to calibrate the indicator fluorescence signals from muscle fibers. For this purpose, either thin wall glass capillaries or quartz capillaries (Vitro Dynamics, New Jersey) filled with the indicator solutions were placed in the same position as the fibers, and the fluorescence signals were measured with conditions identical to those used for the muscle measurements.

In vitro fluorescence excitation spectra were measured at three Mg^{2+} concentrations (0, 20, and 50 mM), and these in vitro spectra were used to calibrate the furaptra spectra obtained in muscle fibers at rest (cf. Fig. 4 *A*). The composition of the in vitro solution was 0–150 mM KCl, 10 mM PIPES (K salt), 0–50 mM $MgCl_2$, 0.2 mM EGTA (ethylene glycol-bis(β-amino-ethyl ether)*N,N,N',N'*-tetraacetic acid), 51 μM furaptra (pH 6.9). The KCl concentration was altered to maintain the solution ionic strength constant at 0.17 M; for example, the solution of highest Mg^{2+} concentration contained 0 mM KCl and 50 mM $MgCl_2$. The low concentration of EGTA (0.2 mM) was included to complex contaminant Ca^{2+}, and the quantity of Mg^{2+} complexed by EGTA was considered negligible (see below). The measured fluorescence excitation spectra had an isosbestic wavelength for Mg^{2+} of 350 nm, a value very close to that observed in previous studies (347 nm, Raju et al., 1989; 348 nm, Konishi et al., 1991). We did not use solutions of intermediate $[Mg^{2+}]$ (between 0 and 20 mM) in this calibration. Instead, we interpolated between 0 and saturating $[Mg^{2+}]$ to obtain the spectrum at intermediate $[Mg^{2+}]$ on the assumption that the spectrum at any $[Mg^{2+}]$ could be expressed as the weighted average of the Mg^{2+}-free and saturating-Mg^{2+} spectra. This assumption was confirmed either on the inverted microscope (at 5 mM $[Mg^{2+}]$) or in a spectrofluorometer (at 1, 2, 5, and 10 mM $[Mg^{2+}]$).

Excitation spectra (not shown) were also measured in Ca^{2+}-free solution (no added Ca^{2+}, 0.2 mM EGTA, 150 mM KCl, 10 mM PIPES) and in saturating-Ca^{2+} solution (20 mM $CaCl_2$, 90 mM KCl, 10 mM PIPES) (pH 6.9). The difference spectrum obtained by subtraction of the Ca^{2+}-free spectrum from the saturating Ca^{2+} spectrum (Fig. 9) was compared with the spectral dependence of in vivo signals obtained during electrically-stimulated activity (cf. fluorescence mode 2 above). The isosbestic wavelength for the Ca^{2+} difference spectrum was 348 nm, a wavelength only slightly shorter than that for Mg^{2+}.

The intracellular concentration of furaptra was estimated by a method similar to that described by Klein, Simon, Szucs, and Schneider (1988). This method is based on a comparison of the fluorescence intensity excited at 350 nm (the isosbestic wavelength for Mg^{2+}) measured in muscle fibers and in thin wall glass capillaries. We therefore measured furaptra's fluorescence intensity in glass capillaries with an internal diameter of 140 μm (the typical fiber diameter in our study) containing solutions of four different indicator concentrations (50, 100, 200, 500 μM) placed in the same position as the muscle. The intensity vs. concentration curve (not shown) was approximately linear up to 200 μM indicator concentration (within a few percent error), but deviated from linearity for the higher concentrations. Thus, the estimate of the indicator concentration was probably less accurate for concentrations higher than 200 μM. Since the fiber diameter varied between 90 and 235 μm, a correction for the fiber diameter was made before the calibration curve was applied. This correction assumed that the fluorescence intensity was linearly related to the square of fiber diameter. This assumption was confirmed in glass capillaries of various internal diameters (50 to 250 μm) containing 100 μM of indicator solution. We also assumed that the indicator molecules are distributed evenly (and exclusively) in the myoplasmic water volume which occupies ~70% of the fiber volume (Baylor et al., 1986). For muscle fibers in which intrinsic absorbance was not measured (and therefore the fluorescence intensity was not corrected for the intrinsic absorbance),

the estimated indicator concentrations are probably underestimated (by ~10%). Our estimates of the indicator concentration may include additional errors, because the indicator molecules probably have a different quantum efficiency in myoplasm than in a salt solution (cf. Konishi et al., 1988).

Some of the characteristics of furaptra's metal-binding reactions were examined in a spectrofluorometer (FP-770; JASCO, Tokyo) by measurement of furaptra's fluorescence excitation spectra in 1 cm quartz cells (16–17°C). For these measurements, the excitation wavelength in 2 nm increments varied between 300 and 450 nm, and an emission wavelength of 510 nm (±5 nm) was selected. The binding reactions of furaptra with Ca^{2+} and Mg^{2+} are very likely to be 1:1 and the indicator K_D's have been previously estimated for Ca^{2+} and Mg^{2+} at 16–17°C (Konishi et al., 1991). As an additional check, we estimated the K_D value for Mg^{2+} based on fluorescence measurements (in place of absorbance measurements used in the previous work; Konishi et al., 1991). The composition of the calibration solutions was identical to those mentioned above for the in vitro fluorescence measurements on the microscope stage (0–150 mM KCl, 10 mM PIPES, 0–50 mM $MgCl_2$, pH 6.9) except for a slightly higher EGTA concentration (0.5 mM) and a low indicator concentration (1 μM). Free Mg^{2+} concentration was calculated from the total added Mg^{2+} minus the concentration calculated to be bound to EGTA. Since the K_D of EGTA for Mg^{2+} is large, 49 mM at 16.5°C (Martell and Smith, 1974), the concentration of Mg^{2+} chelated by EGTA was at most 1% of total added Mg^{2+}. The method of analysis was identical to that employed in the previous work (Konishi et al., 1991); the relative amplitudes of the difference spectra were least-squares fitted to the theoretical 1:1 binding curve with two adjustable parameters: the maximal amplitude of the difference spectrum and the K_D for the 1:1 binding reaction. Two runs, in which [Mg^{2+}] was varied from 0 to 50 mM (8 data points), gave best-fitted K_D values of 5.6 and 5.8 mM. The average value of these two numbers, 5.7 mM, is close to the value obtained previously, 5.3 mM. The slightly higher K_D value obtained here may be due to the slightly higher ionic strength of the calibration solutions used. For the calibration of the furaptra signals in the Results section, we have used the average of the latter two values, 5.5 mM. The K_D value for Ca^{2+} was also checked in similar measurements. In this calibration, the buffer solution (130 mM KCl, 10 mM PIPES, pH 7.0) was passed through a chelex column to minimize the contaminant Ca^{2+}; then $CaCl_2$ was added to set the desired free Ca^{2+} level without the use of an additional Ca^{2+} buffer. A single run in which free Ca^{2+} concentration ([Ca^{2+}]) was varied between 10 μM and 10 mM (furaptra concentration 2 μM, 8 data points) gave a best-fitted K_D of 40 μM, a value close to that obtained previously, 44 μM (Konishi et al., 1991). Since contaminant Ca^{2+} may have been more of a problem in the current measurements, the K_D value obtained in the previous study, 44 μM, was used for the calibration in this study.

Raju et al. (1989) reported pH effects on furaptra's fluorescence excited at 335 and 370 nm in Ca^{2+}- and Mg^{2+}-free condition, and concluded that the apparent pK of furaptra is ~5. In order to obtain more detailed information on the effects of pH changes in the physiological range, we measured fluorescence excitation spectra in 0, 0.5, 5, and 50 mM [Mg^{2+}] at pH 6.5, 6.8, and 7.2 (solution conditions identical to those used for K_D measurements except the pH was adjusted with KOH). At each [Mg^{2+}] level, the furaptra fluorescence excitation spectra obtained at the 3 different pH's were not significantly different. Very similar results were obtained in similar measurements with Ca^{2+}, in which furaptra's fluorescence excitation spectra were measured in 0, 0.04, 0.1, and 20 mM [Ca^{2+}] at pH 6.5, 6.7, 7.0, and 7.2. These results are consistent with the apparent pK of ~5 estimated by Raju et al. (1989), and strongly suggest that pH in the physiological range (6.5–7.2) has little effect on either furaptra's fluorescence or its binding properties to Mg^{2+} and Ca^{2+}.

Statistical tests

The values from more than 2 measurements were expressed as mean ± SEM. For comparison of two data sets, the two-tailed t-test was used ($P < 0.05$).

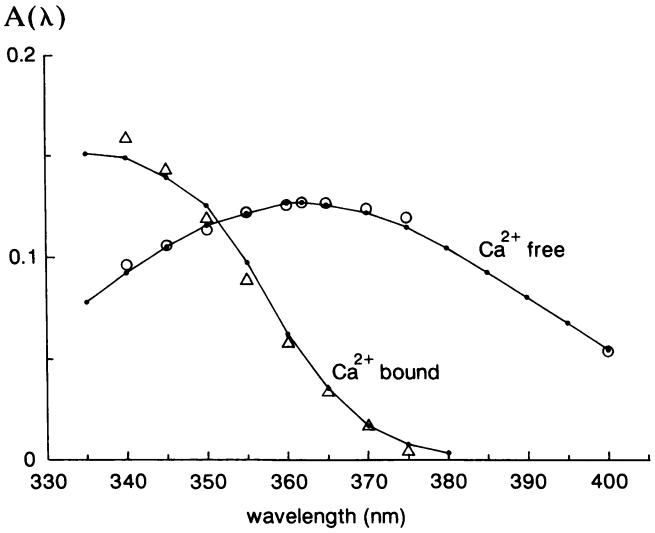

FIGURE 2 Comparison of absorbance spectra of fura-2 measured using a microscope (*symbols*) and in a spectrophotometer (*solid lines*) at 22°C. The microscope measurements were made in thin-walled glass capillaries (inner diameter 160 μm) filled with 250 μM fura-2 solutions (120 mM KCl, 10 mM PIPES, pH 6.9) containing either 2 mM EGTA ("Ca^{2+} free") or 10 mM $CaCl_2$ ("Ca^{2+} bound"). The field of illumination was limited to the central portion (650 μm length and 45 μm width) of the capillary by insertion of a slit (D1 in Fig. 1). An aperture diaphragm (D2 in Fig. 1) was also used to reduce the NA of the objective to 0.3–0.4. For measurements at 340–375 nm or at 400 nm, either a UV transmission filter (transmission band 330–370 nm) or a 400 nm interference filter (half width 10 nm), respectively, was inserted in front of the photodiode (F2 in Fig. 1) in order to eliminate the contamination of fluorescence. The spectrophotometer measurements were made with the sample solutions at 20-fold lower indicator concentration (12.5 μM) in quartz cells of 1 cm path length. Absorbance values obtained in the spectrophotometer were scaled to correct for the differences in indicator concentrations and in optical path lengths.

RESULTS

To check the accuracy of our apparatus for UV absorbance measurements, absorbance spectra of "standard" solutions were measured in capillaries placed on the microscope stage and in a spectrophotometer (Fig. 2). For these measurements, fura-2 (Grynkiewicz et al., 1985), a well characterized Ca^{2+} indicator dye with UV absorbance, was used. For the microscope measurements, the solutions contained 120 mM KCl, 10 mM PIPES, 250 μM fura-2 (pH 6.9) plus either 2 mM EGTA ("Ca^{2+} free form") or 10 mM $CaCl_2$ ("Ca^{2+} bound form"). For the spectrophotometer measurements, which were made with 1 cm cuvettes, the fura-2 concentration was 20-fold less (12.5 μM), in otherwise identical solutions.

After correction for the difference in the fura-2 concentration and optical path lengths (cf. Baylor et al., 1986), the absorbance values obtained on the microscope and in the spectrophotometer agreed within 0.01 absorbance units for wavelengths in the range of 340–375 nm and at 400 nm (Fig. 2). Absorbance values for wavelengths outside this range (shorter than 340 nm and

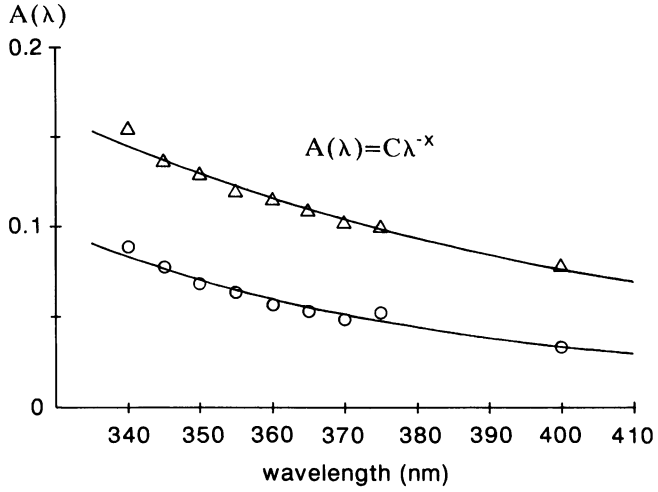

FIGURE 3 Wavelength dependence of intrinsic absorbance measured in two muscle fibers. Absorbance mode recording. (*Circles*) Fiber 021991f1, vertical diameter 105 μm, temperature 16.8–16.9°C. (*Triangles*) Fiber 020691f1, vertical diameter 105 μm, temperature 16.6–16.9°C. Two solid lines represent the best-fitted curve of the functional form $A(\lambda) = C \cdot \lambda^{-X}$ to each muscle data set.

from 380–390 nm) were less reliable (not shown). This is due to the fact that at short wavelengths (<340 nm), the transmission of the optics in the light path (optic fiber, objectives and other lenses) falls steeply, whereas at 380–390 nm, the transmission of the blocking filter (UV-360, F2 in Fig. 1) is low. In either case, the intensity of the light that reached the photo-diode detector (PD in Fig. 1) was below the detection limits considered to give reliable measurements. We therefore restricted the subsequent measurements to the wavelengths 340–375 and 400 nm.

Intrinsic absorbance measurements

Since the fiber absorbance was used for the correction of the fluorescence signal, the light intensity transmitted through muscle fibers was measured before their injection with indicator, at wavelengths between 340 and 375 nm (every 5 nm) and at 400 nm (absorbance mode; see Methods). The muscle fiber was then moved out of the light path by translation of the microscope stage, and light intensity was remeasured at the same wavelengths. The intrinsic absorbance of the fiber at wavelength λ, $A_i(\lambda)$, was calculated as

$$A_i(\lambda) = \log_{10}(I_0/I), \quad (1)$$

where I and I_0 are the light intensities measured with and without the muscle fiber in the optical path, respectively. The intrinsic absorbance measured in two representative muscle fibers is shown in Fig. 3, and the average results from 14 fibers are summarized in Table 1. In each muscle fiber the measured absorbance values were least-squares-fitted by the functional form:

$$A(\lambda) = C \cdot \lambda^{-X}, \quad (2)$$

where $A(\lambda)$ denotes absorbance at wavelength λ, and C and X are arbitrary constants. This functional form has been shown to fit the muscle intrinsic absorbance at longer wavelengths (wavelength 480 to 810 nm) (Baylor et al., 1982, 1986). The average value of the exponent, X, from the 14 muscle fibers shown in Table 1 was 4.1, which was significantly higher than the values 1.1–1.3 (Baylor et al., 1986) and 1.23 (Irving et al., 1987) for visible wavelengths. The larger value of the exponent in our study is consistent with the finding of Baylor et al. (1986) that at 420 nm and 450 nm $A(\lambda)$ changes more steeply with wavelength than predicted from the curve fitted to data points obtained at ≥480 nm. Columns 3 and 4 of Table 1 indicate that the measured absorbance values are in close agreement with those predicted from the curves (at 350 nm, column 3 or at 400 nm, column 4). In the following analysis, the $A(\lambda)$ of the best-fitted (least-squares-fitted) curves were used for the correction of the fluorescence obtained from the same portion of the muscle fiber.

Resting fluorescence spectrum of furaptra

Fig. 4 illustrates the measurement of furaptra's excitation spectrum from resting muscle fibers, and the method used to estimate resting $[Mg^{2+}]$. The fluorescence intensity excited at wavelength λ was measured just before the indicator injection ("background" fluorescence; *closed circles* in Fig. 4 *B*), and this was used as a baseline for the subsequent analysis. The major component of the background fluorescence was the emission from the optical components, which was very stable during the experiments, and a minor component was the autofluorescence of the muscle fiber. After the indicator injection, the fluorescence intensity spectrum was remeasured (*open circles* in Fig. 4 *B*). The furaptra fluorescence excited at wavelength λ (F(λ)) from myoplasm was calculated by subtraction of the closed circles from the open circles. This corrected spectrum is shown as the open circles in part *C*. It is possible that furaptra's fluorescence excitation spectrum from myoplasm (and hence the calibrated $[Mg^{2+}]$) is significantly influenced by the fiber's intrinsic absorbance. Thus a spectrum with an additional correction was obtained (shown as the X's in Fig. 4 *C*), which represents the fluorescence spectrum that would be measured from furaptra if there were no fiber absorbance. For this correction, a slight modification of Eq. 5′ of Baylor, Chandler, and Marshall (1981) was used. At wavelength λ,

$$F' = f \cdot F \quad (3)$$

$$f = \frac{(A_{dye} + A_i) \cdot (1 - 10^{-A_{dye}})}{A_{dye} \cdot (1 - 10^{-(A_{dye}+A_i)})}, \quad (4)$$

where F and F′ denote, respectively, the fluorescence intensity of furaptra with and without the influence of the

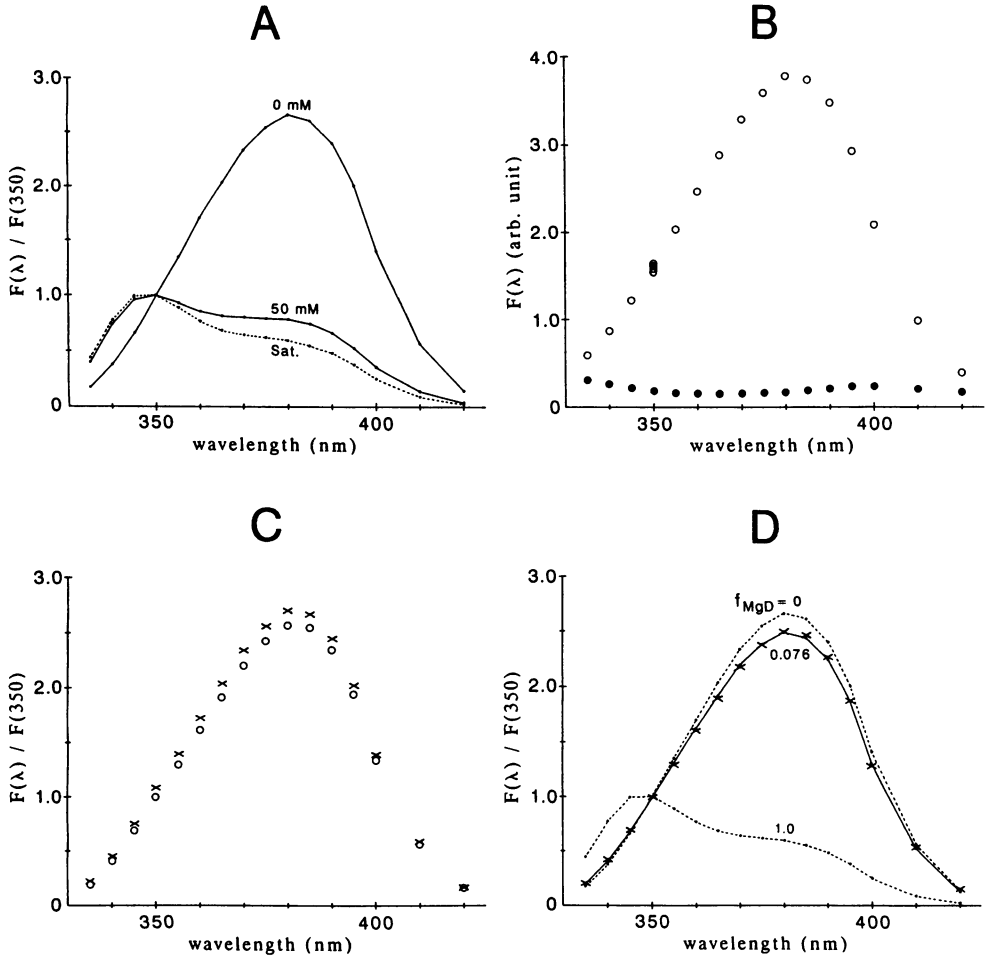

FIGURE 4 Fluorescence excitation spectrum of furaptra obtained in a glass capillary and in a muscle fiber at rest. Fluorescence mode 1 recording. Emission wavelength 500 ± 20 nm. Fiber 021991f1, indicator concentration 75–70 μM. See the legend of Fig. 3 for additional fiber information. (*A*) Fluorescence excitation spectra of 51 μM furaptra obtained in vitro (thin wall glass capillary with 140 μm inner diameter) at 0 mM, 50 mM and saturating [Mg^{2+}] (indicated as 0, 50 and Sat., respectively). The spectrum at saturating [Mg^{2+}] was not measured, but was extrapolated from the spectra at 0 mM, 20 mM (not shown) and 50 mM [Mg^{2+}] with an assumed K_D for Mg^{2+} of 5.5 mM. The spectra were normalized to fluorescence intensity at 350 nm, which is the isosbestic point for Mg^{2+} in our apparatus. 16.7°C. (*B*) "Raw" excitation spectrum obtained from the muscle fiber injected with furaptra (*open circles*) and "background" spectrum measured in the same portion of the muscle fiber just prior to the injection (*closed circles*). Fluorescence intensity at 350 nm was measured four times during the run in order to correct for the time-dependent change in the indicator concentrations, which is mostly due to the diffusion of the indicator away from the injection site. (*C*) (*Open circles*) excitation spectrum of furaptra in the muscle fiber obtained from the "raw" spectrum (*open circles* in part *B*) and the "background" spectrum (*closed circles* in part *B*). The procedure includes (*a*) subtraction of the "background" spectrum from the "raw" spectrum; (*b*) the correction for the time-dependent change in the indicator concentration by linear interpolation between two adjacent measurements at 350 nm excitation; (*c*) normalization to average fluorescence intensity at 350 nm. (X's) excitation spectrum after correction for the fiber's intrinsic absorbance. (*D*) X's, excitation spectrum of furaptra in the fiber corrected for the fiber's absorbance and renormalized to its value at 350 nm. Broken and solid lines are in vitro spectra at three bound fraction of Mg^{2+} (f_{MgD}), as indicated next to the curves. Spectra of f_{MgD} = 0 and 1.0 are the same as those at 0 mM and saturating [Mg^{2+}] in part *A*. The spectrum of f_{MgD} = 0.076 gives the least sum-of-square-errors for the muscle data.

fiber absorbance. f is a correction factor for absorbance and has a value ≥ 1. A_i denotes the fiber's intrinsic absorbance and was estimated as described above. A_{dye}, the absorbance due to the indicator, is a function of the indicator concentration, fiber diameter and the wavelength. For a typical intracellular indicator concentration, 60–70 μM (average value in Table 1), and a path length of 100 μm, the calculated A_{dye} ranged between 0.003 (at 420 nm) and 0.02 (at 370 nm). The exact value of A_{dye}, however, is not critical in the use of Eqs. 3 and 4. For example, with A_i = 0.1 (typical measured value at 350 nm) and a very small value of A_{dye} (e.g., 0.001), f was calculated to be 1.119. On the other hand, with A_i = 0.1 and A_{dye} = 0.1, f was 1.115. Since the difference in the calculated f was very minor, we used a constant A_{dye} of 0.01 for all analyses. In Fig. 4 *C*, the comparison in the measured fluorescence spectrum (*open circles*) and the corrected spectrum (X's) shows, as expected, that the relative amplitude of the correction was larger at shorter wavelengths where the intrinsic absorbance was larger. (Compare, for example, the correction at 355 nm and at 400 nm.)

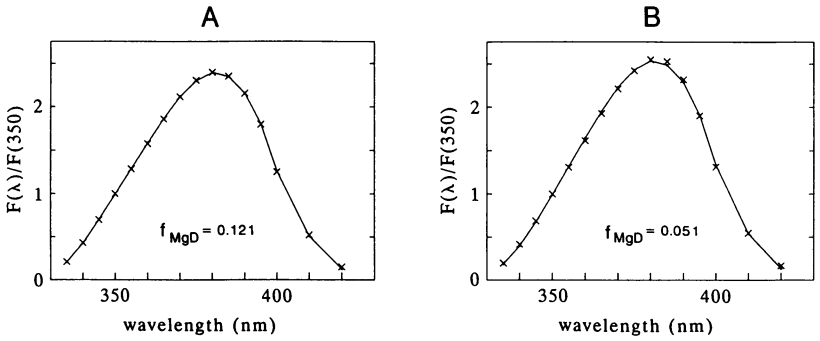

FIGURE 5 Examples of furaptra's fluorescence excitation spectra from two muscle fibers. In parts *A* and *B*, X's are muscle data which have been corrected for the intrinsic absorbance measured in each muscle fiber as shown in Fig. 4. Solid lines in *A* and *B* are the best-fitted in vitro spectra for each muscle data set with the f_{MgD} values indicated near the curves. Fluorescence mode 1 recording. Emission wavelength 500 ± 20 nm. (*A*) Fiber 020691f1, vertical diameter 105 μm, temperature 16.6–16.9°C, indicator concentration 70–63 μM. (*B*) Fiber 020891f1, vertical diameter 145 μm, temperature 16.7–16.9°C, indicator concentration 70–63 μM.

For final analysis, the spectrum obtained after the correction for absorbance was normalized to its value at 350 nm (Fig. 4 *D*, X's). The broken lines in Fig. 4 *D* labeled "f_{MgD} = 0" and "1.0" are the spectra obtained in vitro in Mg^{2+}-free and saturating-Mg^{2+} concentration, respectively, where f_{MgD} denotes the fraction of indicator in the Mg^{2+}-bound form. The muscle data (X's) fell between the two in vitro spectra, but they were much closer to the spectrum of Mg^{2+}-free condition. To obtain a quantitative estimate of f_{MgD} in the resting fiber, the muscle data were least-squares fitted by a linear combination of the Mg^{2+}-free and saturating-Mg^{2+} spectra. From the relative values of the factors that gave the best fit (0.917 and 0.075 for the Mg^{2+}-free and saturating-Mg^{2+} spectra, respectively), 0.076 of the indicator was estimated to be Mg^{2+}-bound. The muscle data were very well fitted by the spectrum of f_{MgD} = 0.076 (the solid line in Fig. 4 *D*) calculated from in vitro spectra. For comparison, f_{MgD} was also estimated from the muscle data without correction for fiber absorbance (*open circles* in Fig. 4 *C*, fit not shown). The best-fitted f_{MgD} value was 0.039. This value is approximately half of that obtained from the corrected spectrum and the fit was worse (twofold greater sum-of-square-errors). Examples of absorbance-corrected spectra from two other muscle fibers, and their fit by the in vitro spectra, are shown in Fig. 5. These spectra are shown as additional representative examples of the very good fit of the muscle data obtained with the in vitro spectra.

From the in vitro K_D of the Mg-furaptra reaction (5.5 mM), the f_{MgD} with the intrinsic absorbance correction was calibrated in terms of $[Mg^{2+}]$ from the usual equation:

$$[Mg^{2+}] = K_D \cdot \frac{f_{MgD}}{1 - f_{MgD}}. \quad (5)$$

Table 1 summarizes the results of this analysis. Columns 6 and 7 give the f_{MgD} values estimated from the uncorrected and corrected data, respectively, from the fibers. In each of 13 muscle fibers, the best-fitted value of f_{MgD} was always larger and the fit was always better after the absorbance correction (the sum-of-square-errors was, on average, smaller by a factor of 2.1). The average f_{MgD} value from column 7 of Table 1, 0.088, is close to 0.1, the value somewhat arbitrarily assumed in the previous study (Konishi et al., 1991). The resting myoplasmic $[Mg^{2+}]$ calibrated from the 12 fibers in part *A* of Table 1 (cf. column 8) ranged from 0.30 to 0.76 mM with an average value of 0.54 mM (K_D assumed to be 5.5 mM). The indicator concentrations during the measurement runs (mean of values at the beginning and at the end of the run; column 5 of Table 1) was, on average, 66 μM; this value is close to 51 μM, the concentration used for the in vitro measurements of calibration spectra. Part *B* of Table 1 shows the results from one muscle fiber in which f_{MgD} was estimated at 16.3–16.4°C in high Mg^{2+}-Ringer's solution, after the fiber was stored at 10–12°C in high Mg^{2+}-Ringer's solution for about 10 h before the optical measurements (Table 1 *B*). The estimated f_{MgD} value was 0.118, which was not markedly different from the values in part *A*.

The analysis described above assumes that the quantity of Ca^{2+}-bound furaptra is negligible in the resting muscle fibers. Estimates of resting myoplasmic $[Ca^{2+}]$ vary according to method but probably do not exceed 0.1 μM (Blinks et al., 1982; Blatter and Blinks, 1991). With a K_D of 48.2 μM for the Ca-furaptra reaction (see below), at most 0.2% of the myoplasmic furaptra would be complexed with Ca^{2+}. This small quantity should not affect the results of the analysis.

Changes in furaptra's fluorescence signals

For the measurements of furaptra's fluorescence change due to changes in $[Mg^{2+}]$ ($\Delta[Mg^{2+}]$), the fluorescence intensities excited at 350 and 380 nm, F(350) and F(380), respectively, were followed with dual-wave-

TABLE 1 **Analysis of absorbance measurements from non-injected fibers and fluorescence measurements from furaptra-injected fibers**

(1)	(2)	(3)	(4)	(5)	(6)	(7)	(8)
	intrinsic absorbance					corrected	
fiber#	X	A(350)	A(400)	[furaptra] (μM)	f_{MgD}	f_{MgD}	[Mg^{2+}] (mM)
A							
012991f1*	3.14	0.156 (0.156)	0.103 (0.108)	165	0.087	0.137	0.87
020691f1	3.91	0.130 (0.129)	0.077 (0.079)	67	0.070	0.121	0.76
020791f1	2.49	0.135 (0.134)	0.097 (0.101)	35	0.042	0.079	0.47
020891f1	7.29	0.050 (0.048)	0.019 (0.020)	67	0.017	0.051	0.30
021491f1	7.55	0.099 (0.099)	0.036 (0.042)	--	--	--	--
021591f1	3.31	0.058 (0.058)	0.037 (0.040)	47	0.046	0.067	0.39
021891f1	4.00	0.081 (0.082)	0.048 (0.054)	67	0.023	0.058	0.34
021891f2	3.06	0.124 (0.120)	0.082 (0.086)	75	0.053	0.093	0.56
021991f1	5.60	0.071 (0.069)	0.034 (0.034)	73	0.039	0.076	0.45
021991f2	3.71	0.122 (0.121)	0.075 (0.078)	85	0.013	0.061	0.36
093091f1	4.21	0.144 (0.145)	0.082 (0.086)	63	0.069	0.121	0.76
093091f2	2.04	0.095 (0.095)	0.072 (0.076)	88	0.094	0.113	0.70
100491f1	3.92	0.079 (0.083)	0.042 (0.048)	85	0.090	0.115	0.71
100991f1	3.04	0.098 (0.098)	0.065 (0.068)	42	0.079	0.106	0.65
mean	4.09	0.103 (0.103)	0.062 (0.066)	66	0.053	0.088	0.54
±S.E.M.	0.44	0.009 (0.009)	0.007 (0.007)	5	0.008	0.008	0.05
N	14	14	14	12	12	12	12
B							
100491f1	2.35	0.088 (0.088)	0.065 (0.067)	88	0.099	0.118	0.71
100991f2	2.25	0.136 (0.136)	0.101 (0.105)	--	--	--	--
101591f1	2.39	0.081 (0.081)	0.059 (0.062)	--	--	--	--
mean	2.33	0.102 (0.102)	0.075 (0.078)				
±S.E.M.	0.04	0.017 (0.017)	0.013 (0.014)				
N	3	3	3				

Column 2 gives the best-fitted exponent, X, in the function form $A(\lambda) = C \cdot \lambda^{-x}$ to the muscle data. Values in columns 3 and 4 are the absorbance values at 350 and 400 nm, respectively, of the best-fitted curves (Measured $A(\lambda)$ values at 350 and 400 nm, respectively, are also shown in parentheses). Columns 5–8 summarize the results of fluorescence excitation spectra of furaptra in resting muscle fibers. Column 5 gives the average indicator concentration during the run estimated from fluorescence intensity at 350 nm excitation in the muscle. Column 6 gives the estimated bound fraction of furaptra to Mg^{2+} (f_{MgD}) in the resting muscle fiber based on spectral data without intrinsic absorbance correction; i.e., the muscle data (for example, *open circles* in Fig. 4 *C*) were not corrected for the intrinsic absorbance and were fitted by linear combination of the in vitro spectra of $f_{MgD} = 0$ and 1.0. Column 7 is the result of improved analysis which includes the correction for fiber's intrinsic absorbance as shown in Fig. 4. Based on f_{MgD} in column 7 and K_D for Mg-furaptra reaction in vitro (5.5 mM), resting Mg^{2+} concentration were calculated and were shown in column 8. (*A*) muscle fibers were in normal Ringer solution for at least 3 h. A fiber 012991f1 (with an asterisk on fiber No.) was dissected and equilibrated in Ringer's solution containing 1 mM Mg^{2+}. The results from this muscle fiber were, therefore, not included in the statistics of fluorescence measurements (columns 5–8). (*B*) muscle fibers were dissected and stored (at 10–12°C) in high Mg^{2+}-Ringer's solution for ~10 h. (The optical measurements were made at 16.3–16.4°C in the high Mg^{2+}-Ringer's solution.)

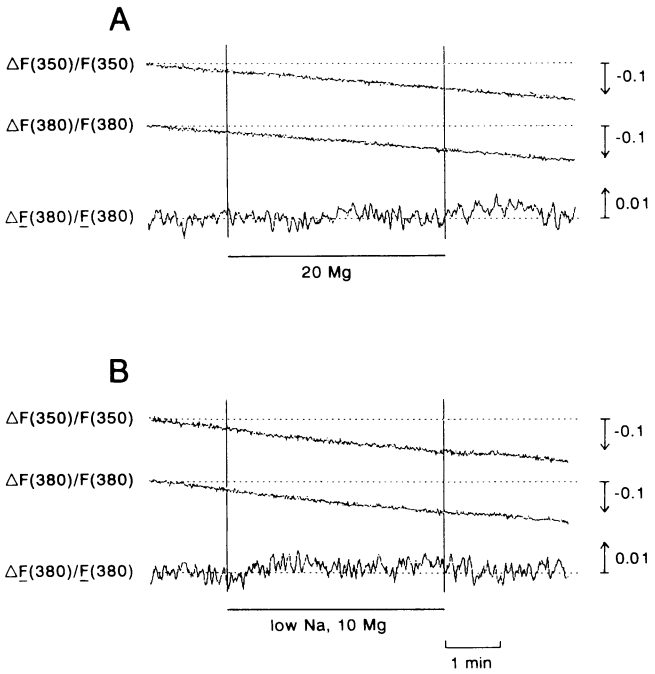

FIGURE 6 Effects of extracellular perfusion by high Mg^{2+}-Ringer's solution (*A*), or low Na^+/Li^+-Ringer's solution (*B*) on furaptra's fluorescence signals. In each panel, the first and second traces show the fractional changes (relative to the first data point) in F(350) and F(380), respectively. The third trace shows the fractional change in F(380). Fluorescence mode 2 recording, dual-wavelength excitation (switching frequency 100 Hz), N.D. 0.5 filter in D1 position (cf. Fig. 1). (*A*) fiber 042691f1, vertical diameter 175 μm, temperature 16.8–16.9°C, indicator concentration 59–52 μM. (*B*) fiber 042691f1, vertical diameter 175 μm, temperature 16.9–17.0°C, indicator concentration 34–30 μM.

length excitation in fluorescence mode 2. Since the myoplasmic indicator concentration in the site of the optical measurement decreased with time after the injection, F(380) was normalized to F(350), the fluorescence intensity excited at the isosbestic wavelength for Mg^{2+}. Because the normalized F(380) (denoted F(380)) is proportional to F(380) per unit indicator concentration, the change in F(380), ΔF(380), should reflect $\Delta[Mg^{2+}]$ independent of the indicator concentration unless the concentration was high enough to cause a significant "inner filter effect." To avoid a large inner filter effect as well as a possible buffering effect of furaptra on $[Mg^{2+}]$ (cf. Konishi et al., 1991), the data obtained with furaptra concentrations of less than 200 μM were principally analyzed.

Fig. 6 shows the results of the experiments in which muscle fibers were perfused with high Mg^{2+}-Ringer's solution (part *A*) or low Na^+/Li^+-Ringer's solution (part *B*). In parts *A* and *B*, both F(350) and F(380) gradually fell with time. F(380), however, showed no significant change (<1%) over the 8 min period shown in Fig. 6 (the F(380) data were expressed as the fractional change in F(380), ΔF(380)/F(380)). Thus, a short term (4 min) perfusion with either 20 mM extracellular Mg^{2+} or low extracellular Na^+ (plus 10 mM Mg^{2+}) caused no detectable change (<1%) in F(380) (and therefore less than 15% change in spatially averaged myoplasmic $[Mg^{2+}]$; see below) in this fiber. Similar results were obtained in all fibers tested, for which the average changes in F(380) at the end of the 4-min perfusion with high Mg^{2+}-Ringer's solution and low Na^+/Li^+-Ringer's solution are, respectively, −0.13 ± 0.05% (8 muscle fibers) and −0.01 ± 0.10% (9 muscle fibers); neither of these changes is detectably different from zero.

Similar experiments were carried out with low Na^+/TMA^+-Ringer's solution (data not shown). Since the application of low Na^+/TMA^+-Ringer's solution caused a twitch-like muscle contraction, possibly due to membrane depolarization, it was impossible to reliably follow F(380) immediately after the application of low Na^+/TMA^+-Ringer's solution. The contraction elicited by this solution, however, was rapidly inactivated, and the recovery from the inactivation took more than several minutes in normal Ringer's solution. We, therefore, employed the following "reversed" protocol: (*a*) The muscle fibers were incubated in low Na^+/TMA^+-Ringer's solution for more than 15 min. The contraction was completely inactivated, and the tension level returned to baseline. (*b*) During the measurement of F(380), the perfusing solution was switched back to normal Ringer's solution. (*c*) After 4-min perfusion of normal Ringer's solution, low Na^+/TMA^+-Ringer's solution was again applied. The second application of low Na^+/TMA^+-Ringer's solution caused no contraction, probably due to the prolonged inactivation. The F(380) value obtained in normal Ringer's solution (at the end of 4-min perfusion) was, then, compared with the average of the before and after values measured in low Na^+/TMA^+-Ringer's solution. The change in F(380) due to low Na^+/TMA^+-Ringer's solution was +0.21 ± 0.10% (3 muscle fibers), which is not significantly different from zero.

In two muscle fibers, F(380) was continuously monitored during an intracellular acidosis initiated by an experimental protocol similar to that shown in Fig. 6. The intracellular acidification was achieved by 5% CO_2, which has been shown to cause a rapid fall in myoplasmic pH by ~0.4 units (cf. Baylor and Hollingworth, 1990). In two experiments, the changes in F(380) at the end of 3 min acid load were +0.28% and +0.33%, values probably not detectably different from zero.

Long-term changes in furaptra's F(380)

In the previous section, we did not detect on a time scale of several minutes any significant change in furaptra's F(380). It was then of interest to know if changes in myoplasmic $[Mg^{2+}]$, i.e., F(380), could be detected on a time scale of hours. Since the indicator concentration in the optical site decreased with time after injection, it was difficult to measure furaptra's fluorescence intensity

from the same muscle fibers for periods longer than about two hours after the indicator injection. We therefore attempted to reduce the rate of diffusion by injecting the furaptra into two or three locations along the muscle fiber separated by 400–500 μm. Multiple injections in a restricted region of the fiber, however, often caused injection damage. In spite of this technical difficulty, five muscle fibers were successfully injected with a sufficient quantity of indicator to allow us to reliably follow the fluorescence signals for 150–260 min. Fig. 7 shows the results obtained from four such experiments. When the muscle fibers were perfused with normal Ringer's solution, F(380) tended to rise linearly on this slow time scale (Fig. 7 *A*). In five muscle fibers, in which the F(380) could be followed for more than an hour (60–175 min), the average slope of the best-fitted lines to the measured F(380) data was +0.65 ± 0.13% per hour (range between +0.21 and +0.92% per hour), if normalized by the value of the *y*-intercept. This average value is significantly different from zero. Since the fibers were incubated in normal Ringer's solution containing nominally no Mg^{2+}, the positive slope of F(380) could be interpreted as a decrease in myoplasmic [Mg^{2+}] as the result of a loss of cell Mg^{2+}. This interpretation, however, may not be valid, because the slope was also found to be positive in three out of four muscle fibers incubated for at least 3 h (range between +0.22 and +0.62% per hour) in the Ringer's solution containing 1 mM Mg^{2+} (the slope in the other muscle fiber was −0.47% per hour). Because the slope was very slight, we did not pursue this question further.

Fig. 7 *B* shows the results from a muscle fiber in which the F(380) was followed for 140 min after the perfusing solution was switched from normal Ringer's solution (containing 0 mM Mg^{2+}) to high Mg^{2+}-Ringer's solution (containing 20 mM Mg^{2+}). The best-fitted slopes for F(380) in normal Ringer's solution and in high Mg^{2+}-Ringer's solution were +0.65% per hour and +0.34% per hour, respectively. In this and four other muscle fibers, in which the F(380) was followed for 60–137 min in the high Mg^{2+}-Ringer's solution, the average slope was +0.60 ± 0.21% per hour, a value not significantly different from that obtained in normal Ringer's solution (+0.65 ± 0.13% per hour). These results, together with the f_{MgD} value within the normal range obtained in one muscle fiber stored for 10 h in the high Mg^{2+}-Ringer's solution (see above), suggest that the change in F(380) caused by 20 mM extracellular [Mg^{2+}] is, if anything, very slight and very slow.

In the experiment shown in Fig. 7 *C*, the perfusion solution was changed from normal Ringer's solution to high Mg^{2+}-Ringer's solution containing 0 mM Ca^{2+} (nominally Ca^{2+} free). The best-fitted slopes for the data in normal Ringer's solution and in high Mg^{2+}-nominally Ca^{2+}-free Ringer's solution were, respectively, +0.87% per hour and −0.37% per hour. Very similar results were obtained in a second fiber, in which the slopes were +0.70% per hour and −0.12% per hour in normal Ringer's solution and the high Mg^{2+}-nominally Ca^{2+} free-Ringer's solution, respectively. Although a definitive conclusion cannot be drawn from these two experiments, the results suggest that any fall in furaptra's

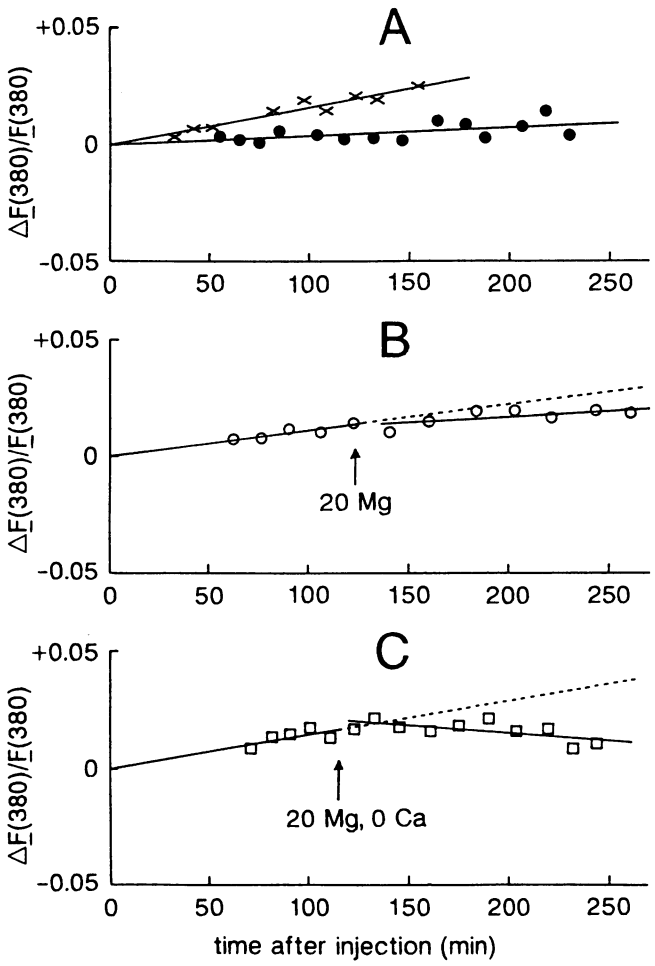

FIGURE 7 Long term observation of furaptra's fluorescence signals (F(380)). Data obtained from two muscle fibers in normal Ringer's solution (*A*), a fiber in which the Ringer' solution was changed (at the *arrow*) to a high Mg^{2+}-Ringer's solution (*B*) and a fiber in which the Ringer was changed (at the *arrow*) to a high Mg^{2+}-nominally Ca^{2+} free-Ringer's solution (*C*). Fluorescence mode 2 recording, dual-wavelength excitation (switching frequency 100 Hz), N.D. 0.5 filter in D1 position (cf. Fig. 1). For each data point, the fiber was illuminated for 3 s by opening the electronic shutter (S1 in Fig. 1), and the signals in the latter 2 s were averaged. (X's) Fiber 051791f1, vertical diameter 150 μm, temperature 16.4–16.6°C, indicator concentration 168–41 μM. (*Closed circles*) Fiber 053191f1, vertical diameter 215 μm, temperature 16.3–16.6°C, indicator concentration 180–26 μM. (*Open circles*) Fiber 051891f1, vertical diameter 175 μm, temperature 16.5–16.7°C, indicator concentration 181–39 μM. (*Squares*) Fiber 060191f2, vertical diameter 180 μm, temperature 16.6–16.7°C, indicator concentration 180–27 μM. For each fiber, F(380) data points in normal Ringer's solution (all points in part *A*, the first 5 points in *B* and *C*) were least-squares fitted by a line (shown in *solid*), and the extrapolated *y*-intercept of the line was taken as zero fractional change. In parts *B* and *C*, the best-fitted lines for data points obtained in the "test" solutions (7 points in *B* and 10 points in *C*) were also shown in solid lines.

F(380) and rise in myoplasmic [Mg^{2+}] in high extracellular Mg^{2+} concentration may be larger in the Ca^{2+} free condition. A similar type of effect was previously suggested for smooth muscle (Nakayama and Tomita, 1990).

In Figs. 6–8, the F(380) data obtained from the muscle fibers were expressed as the fractional change in F(380), $\Delta F(380)/F(380)$. The values of the fractional change in F(380) could be analyzed in terms of $\Delta[Mg^{2+}]$, under the assumption that any fluorescence change in nonstimulated fibers was entirely due to $\Delta[Mg^{2+}]$. The following equations were used for this analysis:

$$\Delta f_{MgD} = (\Delta F(380)/F(380)) \cdot (F(380)/\Delta F_{max}(380)) \quad (6)$$

$$\Delta[Mg^{2+}] = K_D \cdot \frac{\Delta f_{MgD}}{(1 - f_{MgD}) \cdot (1 - f_{MgD} - \Delta f_{MgD})}, \quad (7)$$

where K_D, the dissociation constant assumed for the Mg-furaptra reaction, is 5.5 mM in the in vitro condition (see above). In Eq. 6, Δf_{MgD} is the fraction of the indicator that is driven into the Mg^{2+} bound form by the change in [Mg^{2+}]. $\Delta F_{max}(380)$ denotes the change in F(380) that would be observed if all the indicator molecules were to change from Mg^{2+}-free form to Mg^{2+}-bound form. $\Delta F(380)/F(380)$ was measured in muscle fibers in each experiment, whereas $F(380)/\Delta F_{max}(380)$ was estimated from in vitro measurements:

$$F(380)/\Delta F_{max}(380) = \frac{(1 - f_{MgD} + f_{MgD} \cdot F_{MgD})}{(F_{MgD} - 1)}, \quad (8)$$

where F_{MgD} is the fluorescence intensity (excited at 380 nm) per unit indicator concentration of Mg^{2+}-bound indicator relative to that of Mg^{2+}-free indicator. Since we did not measure absorbance in all experiments (and thus f_{MgD} could not be precisely estimated for each fiber), the average value of f_{MgD} obtained in the previous section, 0.088, was used in combination with the value of F_{MgD}, 0.23, obtained in vitro to calculate $F(380)/\Delta F_{max}(380)$. The calculated value of $F(380)/\Delta F_{max}(380)$, −1.21, was used throughout the analysis.

Given these values, a ±1% change in F(380) corresponds to a Δf_{MgD} of ±0.0121, or a ±13.8% change in the Mg^{2+}-bound fraction relative to f_{MgD} in the resting state (0.088). The $\Delta[Mg^{2+}]$ values for a +1% and a −1% change in F(380) are calculated as −79 μM and +81 μM, respectively, if a K_D of 5.5 mM is assumed. A 1% change in F(380) (therefore ~80 μM $\Delta[Mg^{2+}]$, if K_D is 5.5 mM) is probably marginally larger than the resolution of our system (the smallest detectable change of the signal) which is mainly limited by the noise component of the signal (see Figs. 6–8).

Evidence that F(380) is responsive to myoplasmic [Mg^{2+}]

As the interpretation of the experiments described above depends on furaptra's F(380) signal changing with changes in myoplasmic [Mg^{2+}], we sought direct evidence that F(380) changes with [Mg^{2+}]. For this purpose, either $MgCl_2$ or EDTA (to chelate Mg^{2+}) was injected by micropipette into the myoplasm of furaptra-containing muscle fibers, and furaptra's fluorescence signals were monitored. The $MgCl_2$ (or EDTA) solution was injected into either one or two locations in the fiber regions used for the optical measurements, in order to maximize the local changes in Mg^{2+} concentration. Fig. 8 shows an example of the results obtained in this type of experiment. After the injection of the EDTA solution, the F(380) value increased by about 6% (as expected from the decrease in myoplasmic [Mg^{2+}] due to Mg^{2+}

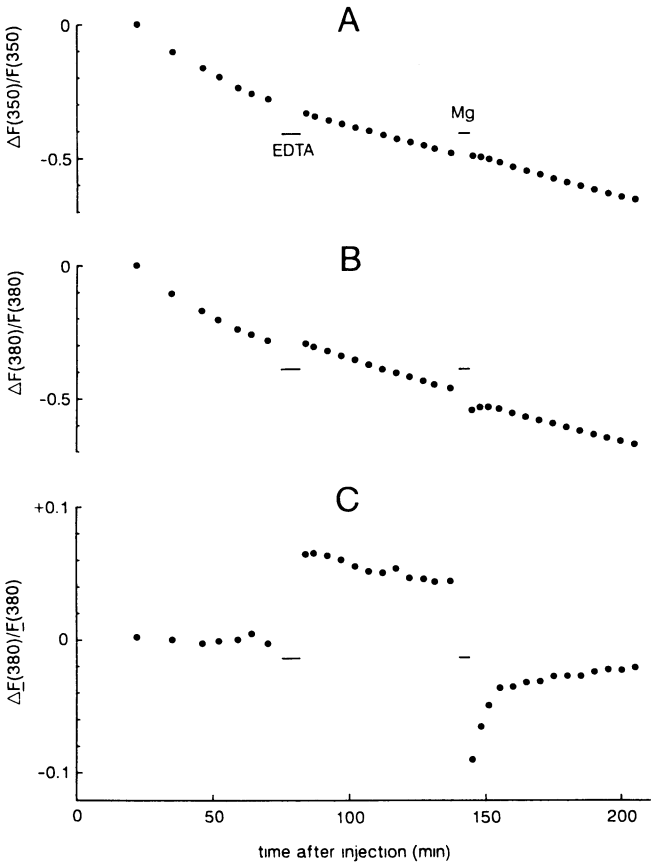

FIGURE 8 Effects of EDTA or $MgCl_2$ injection on furaptra fluorescence signals in a muscle fiber. After injection of furaptra into the fiber (at time 0 on the abscissa), furaptra's fluorescence signals, F(350) and F(380), were followed for ~3 h. 30 mM EDTA (K salt, pH 7.0) and 50 mM $MgCl_2$ (pH 7.0 by 5 mM PIPES) were separately injected into the fiber 70–75 min and 140–142 min, respectively, after the furaptra injection (timing indicated as horizontal bars in parts *A–C*). During either EDTA or $MgCl_2$ injection, fluorescence measurements were interrupted. In parts *A* and *B*, the fractional changes (relative to the first point measured, about 20 min after furaptra injection) in F(350) and F(380), respectively, were plotted as a function of time. In part *C*, the fractional change in F(380) was plotted. Fluorescence mode 2 recording, dual-wavelength excitation (switching frequency 100 Hz), N.D. 0.5 filter was inserted in D1 position (cf. Fig. 1). Fiber 082991f1, vertical diameter 140 μm, temperature 16.4–16.7°C, indicator concentration 421–141 μM.

chelation by EDTA) and this slowly returned towards the baseline. In contrast, the injection of the $MgCl_2$ solution caused a reversal of $\underline{F}(380)$; the $\underline{F}(380)$ fell below the baseline level (as expected from the rise of myoplasmic $[Mg^{2+}]$), and this change then recovered over the next 30–50 min. The recovery after $MgCl_2$ injection seemed to have at least two phases (rapid and slow). Several mechanisms, such as the myoplasmic diffusion of Mg^{2+} out of the optical site, Mg^{2+} extrusion from the cell, and Mg^{2+} binding to myoplasmic binding sites, may underlie the recovery of the change in $[Mg^{2+}]$. An EDTA solution of the same composition injected into another muscle fiber caused an 8% increase in $\underline{F}(380)$. In one muscle fiber, an EDTA solution containing 27 mM EDTA and 0.55 mM furaptra was injected to obtain a rough estimate of myoplasmic EDTA concentration. The rise of furaptra F(350) after injection of the EDTA solution was taken as the measure of the injected amount of furaptra, and the relative concentrations of furaptra and EDTA in myoplasm were assumed to be the same as in the micropipette. About 7 min after the injection, the $\underline{F}(380)$ increased by 6%, and the estimated myoplasmic EDTA concentration was 4.2 mM. The $MgCl_2$ injection was repeated, with similar results, in two other muscle fibers, including one muscle fiber which was injected with a solution containing 50 mM $MgCl_2$ plus 0.5 mM EGTA to eliminate any effects of contaminant Ca^{2+} in the injected solution. Attempts were not made to quantify the amount of injected Mg^{2+}.

Furaptra fluorescence signals during muscle activity

Figure 9 *A* shows fluorescence signals measured at various excitation wavelengths in response to action potential stimulation. Signals such as these have been previously attributed to the myoplasmic $\Delta[Ca^{2+}]$, with little interference from $[Mg^{2+}]$ (Konishi et al., 1991). Since there was little change in fluorescence intensity during activity at 348 nm excitation, the isosbestic wavelength for Ca^{2+} in muscle is probably very close to 348 nm, which is the same isosbestic wavelength observed in vitro. Figure 9 *B* shows a superposition of the $\Delta F(340)$ and $\Delta F(380)$ signals from part *A*, with the $\Delta F(340)$ trace scaled to provide the best fit to the $\Delta F(380)$ trace. The waveforms of both traces were essentially identical, within the noise level, which is expected if the fluorescence signals reflect a single myoplasmic event, e.g., $\Delta[Ca^{2+}]$. Since the Ca^{2+}-dependent fluorescence change is maximal at 380 nm excitation in our experimental set-up, $\Delta F(380)$ was calibrated in terms of $\Delta[Ca^{2+}]$ with the methods analogous to those for $\Delta[Mg^{2+}]$ (see also Eqs. 3 and 4 of Konishi et al., 1991). The equations used (9–11 below) assume that the fraction of indicator bound to Ca^{2+}, f_{CaD}, is zero in the resting state (see above):

$$\Delta f_{CaD} = (\Delta\underline{F}(380)/\underline{F}(380)) \cdot (\underline{F}(380)/\Delta\underline{F}_{max}(380)) \quad (9)$$

$$\Delta[Ca^{2+}] = K_{D,eff} \cdot \frac{\Delta f_{CaD}}{(1 - \Delta f_{CaD})}. \quad (10)$$

In these equations, Δf_{CaD} denotes the fraction of furaptra that is driven into the Ca^{2+}-bound form during activity, and $\Delta\underline{F}_{max}(380)$ is the maximum change in $\underline{F}(380)$ that would be observed if all the indicator molecules were driven into the Ca^{2+}-bound form. $\underline{F}(380)/\Delta\underline{F}_{max}(380)$ was calculated as

$$\underline{F}(380)/\Delta\underline{F}_{max}(380) = \frac{(1 - f_{MgD} + f_{MgD} \cdot F_{MgD})}{F_{CaD} - (1 - f_{MgD} + f_{MgD} \cdot F_{MgD})}, \quad (11)$$

where F_{CaD} denotes the fluorescence intensity per unit indicator concentration of Ca^{2+}-bound form relative to that of Ca^{2+}-free form. With the F_{CaD} and F_{MgD} values of 0.07 and 0.23 obtained in vitro, $\underline{F}(380)/\Delta\underline{F}_{max}(380)$ was calculated to be −1.08. From Δf_{CaD}, $\Delta[Ca^{2+}]$ was calculated by means of Eq. 10, in which $K_{D,eff}$ denotes the effective dissociation constant for Ca-furaptra reaction. From the K_D value obtained in vitro (see above) for the Ca-furaptra reaction in the absence of Mg^{2+} (44 μM) and the average f_{MgD} of 0.088 (corrected f_{MgD} in Table 1), $K_{D,eff}$ was assumed to be 48.2 μM (=44 μM/(1 − f_{MgD})).

In some fibers, $\Delta F(420)$ was analyzed with equations analogous to 9 and 11 in combination with Eq. 10. The values assumed for F_{CaD} and F_{MgD} were 0.02 and 0.17, respectively, which were obtained in vitro at 420 nm excitation.

For the analysis of $\Delta F(380)$ (or $\Delta F(420)$) during muscle activity, the runs with an average indicator concentration of less than 200 μM were used in order to minimize the inner filter effect and the indicator's buffering effect (see above). The results may be compared with those obtained previously from the same type of muscle fibers of the same frog species in very similar experimental conditions (Konishi et al., 1991). The $\Delta[Ca^{2+}]$'s obtained here from 12 muscle fibers showed a very brief time course. The time to peak after stimulation and half-width were 5.6 ± 0.2 ms and 9.3 ± 0.6 ms, respectively, which were essentially the same as the results reported in the previous study (Konishi et al., 1991). There was a quasi-steady-state ΔF signal at later times (ΔF_{steady}, see Fig. 9), which was attributed by Konishi et al. (1991) to two components: (*a*) Mg^{2+} released from parvalbumin in exchange for bound Ca^{2+} and (*b*) a slow tail of $\Delta[Ca^{2+}]$. In 12 runs, $\Delta F_{steady}/\Delta F_{peak}$ (the mean value of ΔF measured 133 to 167 ms after the stimulation was normalized to the peak of ΔF) averaged 0.043 ± 0.010, a value not significantly different from 0.054 ± 0.008, obtained by Konishi et al. (1991). If $\Delta F(380)$ signals were calibrated entirely in terms of $\Delta[Ca^{2+}]$, the peak amplitude was 7.3 ± 0.5 μM. This value is slightly but significantly higher than the value 5.1 ± 0.3 μM calibrated previously from $\Delta F(420)$ signals

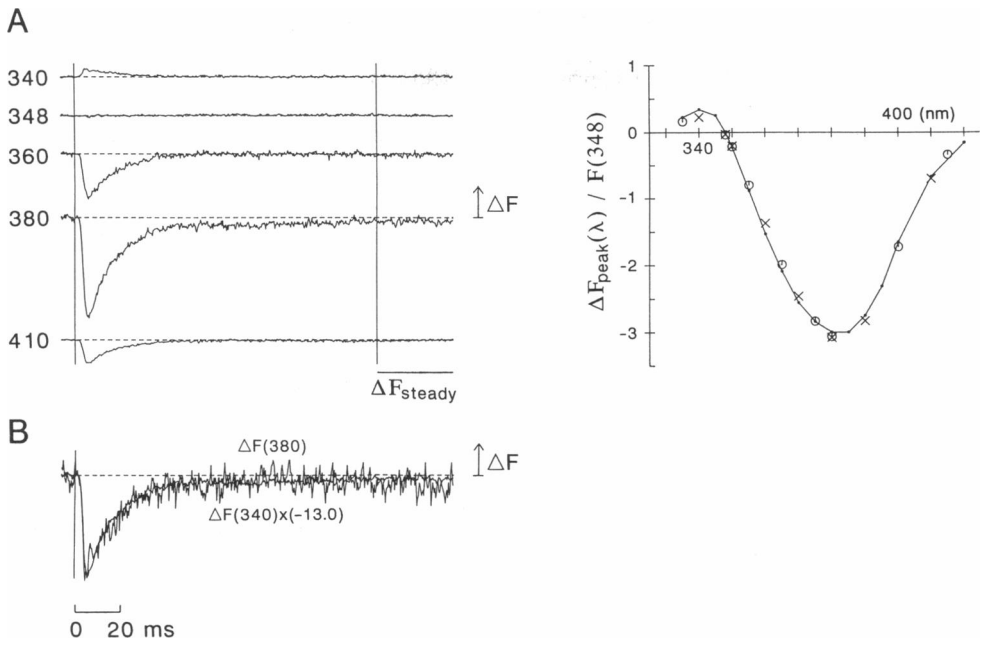

FIGURE 9 (*A*) Furaptra's fluorescence signals (ΔF, in arbitrary units) in response to single action potential at indicated excitation wavelengths (nm) near the trace. The timing of stimulation was indicated by a vertical bar at time 0. Each trace shown is the average of 2–8 sweeps taken sequentially and bracketed by the measurements of F(348). The traces were taken close in time, but have been corrected for the time-dependent change in the indicator concentration using the average of two bracketed F(348) values. (*B*) The comparison of the waveform of fluorescence signals at 340 and 380 nm excitation shown in part *A*. The ΔF(340) signal has been multiplied by −13.0, the best-fitted scaling factor to ΔF(380). Fluorescence mode 2 recording, single-wavelength excitation. Fiber 021891f1, vertical diameter 83 μm, sarcomere length 3.7 μm, temperature 16.7–16.9°C, indicator concentration 60–52 μM during the entire run. Stimulation interval 30 s. (*Right panel*) Comparison of the wavelength dependence of the amplitude of peak ΔF obtained from the experiments of the type shown in part *A* (*open circles* and X 's) and calcium different spectrum obtained in vitro (*small closed circles* connected with *solid lines*). Data from two muscle fibers (different symbols represent different fibers) were scaled to fit the in vitro spectrum. (X 's) fiber 020891f1. For other information, see above. (*Open circles*) Fiber 021591f1, vertical diameter 110 μm, sarcomere length 3.6 μm, temperature 16.8°C, indicator concentration 40–30 μM during the run.

(Konishi et al., 1991). The slight elevation in average $\Delta[Ca^{2+}]$ suggested in the current data is not due to the different excitation wavelengths employed in the two studies, since the peak $\Delta[Ca^{2+}]$ values calibrated from ΔF(380) and ΔF(420) were not significantly different in six muscle fibers in which both ΔF(380) and ΔF(420) signals were measured. (The calibrated peak values in terms of $\Delta[Ca^{2+}]$ were 7.0 ± 0.7 μM and 6.9 ± 0.8 μM, respectively, for ΔF(380) and ΔF(420) signals.) On the other hand, any differences might reflect the difference in the batches of frogs or in the environmental temperature for keeping the frogs (10–12°C for this work and 4°C for Konishi et al. (1991)).

The excitation wavelength dependence of furaptra's fluorescence signals during muscle activity is shown in Fig. 9 (*right*). The wavelength dependence of ΔF_{peak} is very well fitted by the Ca difference spectrum obtained under in vitro conditions. The ΔF_{steady} spectrum was also more or less fitted by the in vitro Ca difference spectrum (not shown), although a detailed comparison was not possible due to the small size of the ΔF_{steady} signal. These results suggest that furaptra responds to myoplasmic $[Ca^{2+}]$ without a significant alteration of its in vitro spectral properties.

DISCUSSION

Intrinsic absorbance of muscle fibers in near UV

In the near UV region, the intrinsic absorbance of muscle fibers was found to be significantly larger and the wavelength dependence was steeper than that previously observed with visible light (Baylor et al., 1986; Irving et al., 1987). The average value of A_i(350) and A_i(400) for fibers with an average diameter of 140 μm were 0.103 and 0.062, respectively. Equivalently the light intensities at 350 and 400 nm were decreased by 21 and 13%, respectively, when incident light was transmitted through the muscle fiber. This level of absorbance could, in some cases, cause significant errors in quantitation of the indicator's fluorescence signals. The correction for the fiber's intrinsic absorbance becomes particularly important if the ion concentration level of interest is far below or above the indicator's K_D (so most of the indicator molecules are in ion-free or in ion-bound form, respectively), as was the case for furaptra in this study. The methods described in this article to correct for the fiber's intrinsic absorbance can be applied to other fluorescence indica-

tors excited in near UV. The results also suggest that the shape of the fluorescence spectrum could be seriously altered in thicker preparations than frog skeletal muscle fibers (e.g., multicellular strips of cardiac or smooth muscles), and that care should be taken in the quantitation of fluorescence signals obtained from such preparations.

Myoplasmic [Mg^{2+}] estimate in muscle fibers at rest

An encouraging finding was that furaptra's fluorescence excitation spectra obtained in frog skeletal muscle, throughout the entire range of scanned wavelengths, were well fitted by calibration spectra obtained under in vitro conditions. In particular, there was no indication of a spectral shift for fibers (either at rest or during activity), as was observed in the case of either absorbance or fluorescence spectra from other indicator dyes (e.g., antipyrylazo III (Baylor et al., 1986), phenol red (Baylor and Hollingworth, 1991), indo-1 (Popov et al., 1988), and possibly fura-2 (Klein et al., 1988). The unaltered spectral properties of furaptra may be related to the relatively small percentage, 42–51%, of furaptra bound to myoplasmic constituents (cf. antipyrylazo III (≃75%), phenol red (≃80%) and fura-2 (≃75%)).

From the corrected f_{MgD}'s obtained from furaptra, a straightforward calibration with the K_D value obtained in vitro (5.5 mM for Mg^{2+}) implies an average myoplasmic [Mg^{2+}] of 0.54 mM. This calibration assumes however that the K_D of the indicator for Mg^{2+} is unaltered by myoplasm. However, it has been suggested that fura-2, a Ca^{2+} indicator structurally-related to furaptra, reacts with Ca^{2+} with a nearly fourfold larger K_D when bound to aldolase (Konishi et al., 1988); the effect of protein binding on fura-2's K_D appears to be common among other protein species as well (BSA, creatine kinase, lactic dehydrogenase and glutalaldehydephosphate dehydrogenase) (Uto et al., 1991). Thus, the calibrated myoplasmic [Mg^{2+}] should be considered as a lower limit, if the K_D for Mg^{2+} of bound furaptra is altered in a similar fashion as that of bound fura-2 for Ca^{2+}. Since ~40–50% of furaptra appears to be bound to relatively immobile myoplasmic constituents, as estimated from its myoplasmic diffusion (Konishi et al., 1991), the in vivo K_D values for Ca^{2+} and Mg^{2+} may be greater by a factor of two than those observed in vivo. A factor-of-two correction appears to be reasonable for the calibration of furaptra's fluorescence signals during muscle activity in terms of $\Delta[Ca^{2+}]$ (Konishi et al., 1991). Thus, the corrected estimate of myoplasmic [Mg^{2+}] as obtained from a corrected calibration is ~1.1 mM (= 0.54 mM × 2). This value is in reasonable agreement with recent estimates of myoplasmic [Mg^{2+}] in resting frog skeletal muscle: 0.93 mM (in Ringer's solution containing 1 mM Mg^{2+}) by the Mg^{2+}-sensitive electrode with a new sensor ETH-5214 (Blatter, 1990); 0.80 mM (in normal Ringer's solution) and 1.69 mM (in 1 mM Mg^{2+} containing Ringer's solution) by the Mg^{2+}-electrode employing an ETH-1117 sensor (Alvarez-Leefmans et al., 1986); about 0.6 mM by ^{31}P-NMR (Gupta and Gupta, 1984). A theoretical calculation based on the biochemical literature also supported the [Mg^{2+}] value of around 0.8 mM (Godt and Maughan, 1988). These and other estimated values, however, should be considered tentative, because each method has significant intrinsic problems. The Mg^{2+}-sensitive electrodes, particularly those employing the sensor ETH-1117, have considerable interference from K^+ and Na^+. The estimated [Mg^{2+}] values (in frog skeletal muscle) with ETH-1117 tend to be high (3.3 mM by Hess et al. (1982) and 3.8 mM by López, Alamo, Caputo, Vergara and DiPolo (1984)) probably for this reason (if the correction for the interference is not made). The relatively recent Mg^{2+} sensor, ETH-5214, is reported to have much better selectivity over K^+, Na^+ and H^+ (Blatter, 1990), but the estimated myoplasmic [Mg^{2+}] values show large scattering in the report of Blatter (1990) (ranging from 0.1–4.4 mM according to Blatter and Blinks, 1991), which may be compared with that in this study (ranging from 0.30–0.76 mM, Table 1).

^{31}P-NMR methods, on the other hand, critically rely on the availability of a precise K_D for the binding of Mg^{2+} to ATP. The large variations of estimated myoplasmic [Mg^{2+}] were partly due to the different values used for K_D of MgATP (Garfinkel and Garfinkel, 1984), but other difficulties have also been pointed out; pH dependence of the Mg^{2+}-ATP reaction and its K_D value being far below the [Mg^{2+}] encountered in myoplasm. The latter follows that the formation of MgATP is close to saturation in the physiological condition (for review, see London, 1991).

Attempts have also been made to estimate the resting myoplasmic [Mg^{2+}] with metallochromic indicator dyes. However, for a myoplasmic pH of 6.9, quite varied estimates were obtained with different dyes: 1.2–3.5 mM from arsenazo III (Baylor et al., 1982; Close and Lännergren, 1984; Baylor et al., 1986), 0.3 mM from dichlorophosphonazo III (Baylor et al., 1982), 4.4–6 mM from arsenazo I (Baylor et al., 1982; Konishi et al., 1989), 0.8–1.7 mM from antipyrylazo III (Baylor et al., 1986). Apart from a rather strong pH dependence of the metallochromic indicators, the variations may also be attributed to altered properties of the indicator(s) inside muscle fibers (Baylor et al., 1982). It was found that these and most of the other indicators, when injected into myoplasm, appeared to be heavily bound to large myoplasmic molecules, and this binding could cause alterations in the indicator's optical and chelating properties (e.g., Konishi et al., 1988). Although furaptra was found to be somewhat less bound to cellular constituents in myoplasm, the effects of myoplasmic binding cannot be disregarded in the quantitation of the fluorescence signals (see above for the twofold correction of K_D). In

spite of the lack of any apparent spectral shift obtained in muscle fibers, we cannot exclude the possibility that there are multiple populations of furaptra molecules bound to various cell constituents which have different spectral shifts (e.g., red shifts and the blue shifts of different degrees; cf. Ishijima et al., 1991) might cancel each other to fortuitously make the overall spectrum unshifted. However, until a more complete understanding of the properties of bound furaptra molecules is obtained, the value of 1.1 mM obtained in this study for the resting myoplasmic $[Mg^{2+}]$ equilibrated in normal Ringer's solution is probably a reasonable one.

The absence of rapid change in resting $[Mg^{2+}]$

The fluorescence signal related to resting myoplasmic $[Mg^{2+}]$, F(380), did not change significantly by short term (4 min) extracellular perfusion of either the 20 mM Mg^{2+} solution or the low Na^+ plus 10 mM Mg^{2+} solution. This result is clearly contradictory to the reported results obtained with a Mg^{2+}-sensitive electrode (Blatter, 1990), in which rapid and reversible changes in $[Mg^{2+}]$-related electrode signal were detected in similar experimental conditions in the identical tissue specimen of the same frog species. The amplitude of the changes in $[Mg^{2+}]$ reported by Blatter (1990), 61–127% of resting $[Mg^{2+}]$, is considered to be at least 4–8 times larger than the resolution of our system (see above). It is important to consider possible ways (apart from the slight differences in solutions) in which this discrepancy could have arisen.

The furaptra measurements might conceivably have been influenced by binding of the indicator molecules to myoplasmic constituents (see above). This raises the possibility that furaptra, when introduced into myoplasm, binds Mg^{2+} with very low affinity (e.g., ten times higher K_D, 55 mM), and only undergoes a small change in fluorescence (below the noise level) in response to a significant change in $[Mg^{2+}]$. For this explanation, however, one has to assume one of the two following situations (or the combination of the two) to be consistent with the non-zero f_{MgD} (on average, 0.088) obtained from the muscle fibers: (case 1) Resting myoplasmic $[Mg^{2+}]$ is high (5.4 mM with 10 times higher K_D). (case 2) The true value f_{MgD} in myoplasm is very close to zero, and the difference in the spectral shape between the muscle spectra and the Mg^{2+}-free spectrum in vitro is an artifact of some kind (e.g., altered spectral shape due to the indicator binding to large myoplasmic molecules, not to Mg^{2+}). Although we cannot completely rule out these possibilities, it is unlikely that furaptra's K_D for Mg^{2+} in myoplasm is an order of magnitude higher than that in vitro for the following reasons: (*a*) The injection of 4 mM myoplasmic EDTA caused a large change in the fluorescence signal which was probably related to a reduction of myoplasmic $[Mg^{2+}]$. The apparent reduction of myoplasmic $[Mg^{2+}]$ by EDTA injection is a particularly strong argument against case 2. (*b*) The late phase of furaptra fluorescence signals during muscle activity (ΔF_{steady}, Fig. 9) is well explained by Mg^{2+} released from parvalbumin if the K_D for Mg^{2+} is assumed to be 2–3 times higher in myoplasm than in vitro (Konishi et al., 1991). (*c*) Furaptra's K_D for Ca^{2+} appears to be altered in myoplasm by a factor of only two, not ten (Konishi et al., 1991). The existence of myoplasmic Ca^{2+} transients of relatively large size and the fast time course during muscle activity also strongly argues against the possibility that intracellularly injected furaptra is trapped in some compartment which is not easily accessible from myoplasm.

One possible methodological impediment in the measurements reported using the Mg^{2+}-sensitive electrodes may be the sustained impalement of the membrane (usually by two, in some cases three electrodes) during ion measurements, which could be the cause of the leakage at the sites of impalement (Blatter and Blinks, 1991). This could erroneously cause a localized increase of $[Mg^{2+}]$, particularly in the high Mg^{2+} solutions, although the leakage alone cannot explain the considerable change in $[Mg^{2+}]$-related electrode signal under Na^+-free conditions reported by Blatter (1990). (There are also slight differences in the solution compositions used in the two studies, although their contribution is unclear. We kept the osmolality of the high Mg^{2+}-Ringer's solution the same as that of normal Ringer's solution, but Blatter (1990) probably did not (at least not described in the paper). Our low Na^+ solution contained 10 mM Mg^{2+}, compared with 1 mM Mg^{2+} in the solution used by Blatter (1990).)

Finally, the difference in the results obtained with furaptra and Mg^{2+}-selective microelectrodes might result from the fact that two methods measure different things. The furaptra fluorescence signal presumably reflects the spatially averaged myoplasmic $[Mg^{2+}]$, whereas the Mg^{2+}-sensitive electrode senses $[Mg^{2+}]$ only at the tip which is no more than a few microns away from the cell surface. It is, therefore, possible that two methods (furaptra and the Mg^{2+} electrode) both measure the true change in $[Mg^{2+}]$ in different locations, if a significant radial gradient of $[Mg^{2+}]$ concentration is formed in high extracellular $[Mg^{2+}]$ or low extracellular $[Na^+]$. Future studies of fluorescence imaging (Westerblad et al., 1990) may elucidate this problem.

The experimental results, thus far obtained, on the existence and importance of the Na^+/Mg^{2+} exchanger are contradictory in various tissues, such as squid giant axon (Baker and Crawford, 1972), barnacle muscle (Ashley and Ellory, 1972) and heart cells (Murphy et al., 1989; Buri and McGuigan, 1990). Our results in frog skeletal muscle fibers are not consistent with the Na^+/Mg^{2+} exchanger as an important Mg^{2+} transporter.

The slow change in myoplasmic [Mg^{2+}]

When a muscle fiber was incubated in high extracellular [Mg^{2+}], we did not detect a significant rise in myoplasmic [Mg^{2+}] at least for 60 min. Although there was a slight suggestion of slow rise of myoplasmic [Mg^{2+}] over a period of 2–3 h, the results indicate that myoplasmic [Mg^{2+}] is very stably maintained for hours even in high extracellular Mg^{2+}. Since a large electrochemical gradient favors Mg^{2+} influx across the cell membrane, the constant (or nearly constant) level of myoplasmic [Mg^{2+}] presumably results from one (or both) of the following mechanisms (*a*) a very low permeability of the cell membrane for Mg^{2+}, (*b*) an efficient transport system for extruding Mg^{2+}. In frog skeletal muscle fibers, experimental results obtained by atomic absorption spectroscopy (O'Donnell and Kovács, 1974; Ling et al., 1979) and Mg^{2+}-electrodes with ETH-1117 as a sensor (Alvarez-Leefmans et al., 1986) also suggest a slow gain of intracellular Mg^{2+} content in high extracellular Mg^{2+} conditions. It seems important for future investigations to carry out detailed studies on the long term change in myoplasmic [Mg^{2+}].

In conclusion, the spatially averaged myoplasmic [Mg^{2+}] in frog skeletal muscle fibers is estimated to be ~1 mM. On a time scale of minutes, the [Mg^{2+}] level appears to be stably maintained, independent of extracellular [Mg^{2+}], extracellular [Na^+] and intracellular acidosis. It is, thus, unlikely that cellular functions are regulated by changes in myoplasmic [Mg^{2+}] on this time scale for these experimental conditions. We do not, however, exclude the possibility that the change in the Mg^{2+} affinity of the regulatory site may play an important role, as hypothesized by Lamb and Stephenson (1991).

While this paper was under review, Westerblad and Allen (1992) reported measurements of myoplasmic [Mg^{2+}] with furaptra in mouse skeletal muscle. The estimated myoplasmic [Mg^{2+}] value from F(340)/F(360) ratio was ~0.8 mM. They found that, within 5 min, the myoplasmic [Mg^{2+}] was unchanged by removal of extracellular Na^+, and was only marginally changed in 20 mM extracellular [Mg^{2+}] (Δ[Mg^{2+}], +86 μM) or intracellular alkalization (Δ[Mg^{2+}], −65 μM). Interestingly, amphibian and mammalian skeletal muscle cells seem to have similar features on myoplasmic [Mg^{2+}] (resting [Mg^{2+}] level and its stringent regulation), at least at ~20°C. It is not clear at this point, however, if the mechanism responsible for the regulation of the myoplasmic [Mg^{2+}] are common in amphibian and mammalian skeletal muscles.

We thank Drs. S. M. Baylor and J. R. Berlin for helpful comments on the manuscript, Dr. M. Nishimuta for estimation of contaminant Ca^{2+} in the solution with atomic absorption spectrophotometry, and Ms. M. Shibuya for editing the manuscript.

This work was supported by grant No. 03670043 from the Ministry of Education, Science and Culture (Japan), and a Japan Heart Foundation Research Grant for 1991 to M. Konishi.

Received for publication 1 June 1992 and in final form 31 August 1992.

REFERENCES

Alvarez-Leefmans, F. J., S. M. Gamiño, F. Giraldez, and H. González-Serratos. 1986. Intracellular free magnesium in frog skeletal muscle fibres measured with ion-selective microelectrodes. *J. Physiol. (Lond.)*. 378:461–483.

Ashley, C. C., and J. C. Ellory. 1972. The efflux of magnesium from single crustacean muscle fibres. *J. Physiol. (Lond.)*. 226:653–674.

Baker, P. F., and A. C. Crawford. 1972. Mobility and transport of magnesium in squid giant axons. *J. Physiol. (Lond.)*. 227:855–874.

Baylor, S. M., W. K. Chandler, and M. W. Marshall. 1981. Studies in skeletal muscle using optical probes of membrane potential. *In* The Regulation of Muscle Contraction: Excitation-Contraction Coupling. A. D. Grinnell and M. A. B. Brazier, editors. Academic Press, New York. 97–130.

Baylor, S. M., W. K. Chandler, and M. W. Marshall. 1982. Optical measurements of intracellular pH and magnesium in frog skeletal muscle fibres. *J. Physiol. (Lond.)*. 331:105–137.

Baylor, S. M., S. Hollingworth, C. S. Hui, and M. E. Quinta-Ferreira. 1986. Properties of the metallochromic dyes arsenazo III, antipyrylazo III and azo 1 in frog skeletal muscle fibres at rest. *J. Physiol. (Lond.)*. 377:89–141.

Baylor, S. M., and S. Hollingworth. 1990. Absorbance signals from resting frog skeletal muscle fibers injected with the pH indicator dye, phenol red. *J. Gen. Physiol.* 96:449–471.

Blatter, L. A. 1990. Intracellular free magnesium in frog skeletal muscle studied with a new type of magnesium-selective microelectrode: interactions between magnesium and sodium in the regulation of $[Mg^{2+}]_i$. *Pflügers Arch.* 416:238–246.

Blatter, L. A., and J. R. Blinks. 1991. Simultaneous measurement of Ca^{2+} in muscle with Ca electrodes and aequorin. Diffusible cytoplasmic constituent reduces Ca^{2+}-independent luminescence of aequorin. *J. Gen. Physiol.* 98:1141–1160.

Blinks, J. R., W. G. Wier, P. Hess, and F. G. Prendergast. 1982. Measurement of Ca^{2+} concentrations in living cells. *Prog. Biophys. Mol. Biol.* 40:1–114.

Buri, A., J. A. S. McGuigan. 1990. Intracellular free magnesium and its regulation, studied in isolated ferret ventricular muscle with ion-selective microelectrodes. *Exp. Physiol.* 75:751–761.

Close, R. I., and J. I. Lännergren. 1984. Arsenazo III calcium transients and latency relaxation in frog skeletal muscle fibres at different sarcomere lengths. *J. Physiol. (Lond.)*. 355:323–344.

Donaldson, S. K. B., and W. G. L. Kerrick. 1975. Characterization of the effects of Mg^{2+} on Ca^{2+}- and Sr^{2+}-activated tension generation of skinned skeletal muscle fibers. *J. Gen. Physiol.* 66:427–444.

Endo, M. 1977. Calcium release from the sarcoplasmic reticulum. *Physiol. Rev.* 57:71–108.

Flatman, P. W. 1984. Magnesium transport across cell membranes. *J. Membr. Biol.* 80:1–14.

Garfinkel, L., and D. Garfinkel. 1984. Calculation of free-Mg^{2+} concentration in adenosine 5′-triphosphate containing solutions in vitro and in vivo. *Biochemistry.* 23:3547–3552.

Gillis, J. M., D. Thomason, J. Lefèvre, and R. H. Kretsinger. 1982. Parvalbumins and muscle relaxation: a computer simulation study. *J. Muscle Res. Cell Motil.* 3:377–398.

Godt, R. E., and D. W. Maughan. 1988. On the composition of the cytosol of relaxed skeletal muscle of the frog. *Am. J. Physiol.* 254:C591–C604.

Grynkiewicz, G., M. Poenie and R. Y. Tsien. 1985. A new generation of Ca^{2+} indicators with greatly improved fluorescence properties. *J. Biol. Chem.* 260:3440–3450.

Gupta, R. K., and P. Gupta. 1984. NMR studies of intracellular metal ions in intact cells and tissues. *Annu. Rev. Biophys. Bioeng.* 13:221–246.

Hess, P., P. Metzger, and R. Weingart. 1982. Free magnesium in sheep, ferret and frog striated muscle at rest measured with ion-selective micro-electrodes. *J. Physiol. (Lond.)*. 333:173–188.

Inesi, G. 1985. Mechanism of calcium transport. *Annu. Rev. Physiol.* 47:573–601.

Irving, M., J. Maylie, N. L. Sizto, and W. K. Chandler. 1987. Intrinsic optical and passive electrical properties of cut frog twitch fibers. *J. Gen. Physiol.* 89:1–14.

Ishijima, S., T. Sonoda, and M. Tatibana. 1991. Mitogen-induced early increase in cytoplasmic free Mg^{2+} concentration in single Swiss 3T3 fibroblasts. *Am. J. Physiol.* 261:C1074–1080.

Klein, M. G., B. J. Simon, G. Szucs, and M. F. Schneider. 1988. Simultaneous recording of calcium transients in skeletal muscle using high and low affinity calcium indicators. *Biophys. J.* 53:971–988.

Konishi, M., A. Olson, S. Hollingworth, and S. M. Baylor. 1988. Myoplasmic binding of fura-2 investigated by steady-state fluorescence and absorbance measurements. *Biophys. J.* 54:1089–1104.

Konishi, M., P. C. Pape, S. Hollingworth, and S. M. Baylor. 1989. Myoplasmic absorbance signals from arsenazo I, a pH/Mg^{2+} indicator dye. *Biophys. J.* 55:412*a*. (Abstr.)

Konishi, M., S. Hollingworth, A. B. Harkins, and S. M. Baylor. 1991. Myoplasmic calcium transients in intact frog skeletal muscle fibers monitored with the fluorescent indicator furaptra. *J. Gen. Physiol.* 97:271–301.

Konishi, M., N. Suda, and S. Kurihara. 1992. Myoplasmic free magnesium concentration in frog skeletal muscle fibers at rest. *Jpn. J. Physiol.* In press.

Lamb, G. D., and D. G. Stephenson. 1991. Effect of Mg^{2+} on the control of Ca^{2+} release in skeletal muscle fibres of the toad. *J. Physiol. (Lond.)*. 434:507–528.

Ling, G. N., C. Walton, and M. R. Ling. 1979. Mg^{++} and K^{+} distribution in frog muscle and egg: a disproof of the Donnan theory of membrane equilibrium applied to the living cells. *J. Cell Physiol.* 101:261–278.

London, R. E. 1991. Methods for measurement of intracellular magnesium: NMR and fluorescence. *Annu. Rev. Physiol.* 53:241–258.

López, J. R., L. Alamo, C. Caputo, J. Vergara, and R. DiPolo. 1984. Direct measurement of intracellular free magnesium in frog skeletal muscle using magnesium-selective microelectrodes. *Biochim. Biophys. Acta.* 804:1–7.

Martell, A. E., and R. M. Smith. 1974. Critical Stability Constants. Vol. 1: Amino Acids, Plenum Publishing Corp., New York. 199–269.

Murphy, E., C. C. Freudenrich, L. A. Levy, R. E. London, and M. Lieberman. 1989. Monitoring cytosolic free magnesium in cultured chicken heart cells by use of the fluorescent indicator furaptra. *Proc. Natl. Acad. Sci. USA.* 86:2981–2984.

Nakayama, S., and T. Tomita. 1990. Regulation of intracellular free magnesium concentration in the taenia of guinea-pig caecum. *J. Physiol. (Lond.)*. 435:559–572.

O'Donnell, J. M., and T. Kovács. 1974. Functional and ionic changes accompanying magnesium penetration in skeletal muscle. *Pflügers Arch.* 350:321–334.

Popov, E. G., I. Y. Gavrilov, E. Y. Pozin, and Z. A. Gabbasov. 1988. Multiwavelength method for measuring concentration of free cytosolic calcium using the fluorescent probe indo-1. *Arch. Biochem. Biophys.* 261:91–96.

Raju, B., E. Murphy, L. A. Levy, R. D. Hall, and R. E. London. 1989. A fluorescent indicator for measuring cytosolic free magnesium. *Am. J. Physiol.* 256:C540–C548.

Suda, N., and S. Kurihara. 1991. Intracellular calcium signals measured with fura-2 and aequorin in frog skeletal muscle fibers. *Jpn. J. Physiol.* 41:277–295.

Uto, A., H. Arai, and Y. Ogawa. 1991. Reassessment of fura-2 and the ratio method for determination of intracellular Ca^{2+} concentrations. *Cell Calcium.* 12:29–37.

Westerblad, H., and D. G. Allen. 1992. Myoplasmic free Mg^{2+} concentration during repetitive stimulation of single fibres from mouse skeletal muscle. *J. Physiol. (Lond.)*. 453:413–434.

Westerblad, H., J. A. Lee, A. G. Lamb, S. R. Bolsover, and D. G. Allen. 1990. Spatial gradients of intracellular calcium in skeletal muscle during fatigue. *Pflügers Arch.* 415:734–740.